ISTANBUL TECHNICAL UNIVERSITY ★ INSTITUTE OF SCIENCE AND TECHNOLOGY

NANOTEMPLATE FORMATION ON INORGANIC SUBSTRATES BY USING SURFACE LAYER PROTEINS

M.Sc. Thesis by

Zehra Beril AKINCI

Department: Metallurgical and Materials Engineering

Programme: Materials Engineering

MAY 2007

İSTANBUL TEKNİK ÜNİVERSİTESİ ★ FEN BİLİMLERİ ENSTİTÜSÜ

İNORGANİK YÜZEYLERDE HÜCRE DUVAR PROTEİNLERİ İLE ORGANİK NANOYAPILARIN OLUŞTURULMASI

YÜKSEK LİSANS TEZİ

Zehra Beril AKINCI

(506051420)

Tezin Enstitüye Verildiği Tarih : 7 Mayıs 2007

Tezin Savunulduğu Tarih : 18 Haziran 2007

Tez Danışmanları : Prof. Dr. Mustafa ÜRGEN

Doç. Dr. Candan TAMERLER BEHAR

Diğer Jüri Üyeleri: Yard. Doç. Dr. Nevin Gül KARAGÜLER (İ.T.Ü.)

Doç. Dr. Kürşat KAZMANLI (İ.T.Ü.)

Doç. Dr. Gültekin GÖLLER (İ.T.Ü.)

MAYIS 2007

ISTANBUL TECHNICAL UNIVERSITY ★ INSTITUTE OF SCIENCE AND TECHNOLOGY

NANOTEMPLATE FORMATION ON INORGANIC SUBSTRATES BY USING SURFACE LAYER PROTEINS

M.Sc. Thesis by

Zehra Beril AKINCI

(506051420)

Date of submission : 7 May 2007

Date of defence examination: 18 June 2007

Supervisor (Chairman): Prof. Dr. Mustafa ÜRGEN

Assoc. Prof. Candan TAMERLER BEHAR

Members of the Examining Committee: Assist.Prof. Dr. Nevin Gül KARAGÜLER (I.T.U.)

Assoc. Prof. Dr. Kürşat KAZMANLI (I.T.U.)

Assoc. Prof. Dr. Gültekin GÖLLER (I.T.U.)

MAY 2007

ACKNOWLEDGEMENTS

I am sincerely thankful to Professor Mustafa Ürgen and Associate Professor Candan Tamerler Behar, my advisors, for their guidance, advice, criticism and endless encouragement. Their enthusiasm for science, teaching and learning has changed definitively my view of science and research.

I would like to thank to Professor Mehmet Sarıkaya for getting me acquainted with molecular biomimetics and supporting my study with his advices.

I would like to send my special thanks to Senem Donatan for providing me with both, technical and endless moral support in every single moment during my study, for sharing all her knowledge with me and especially for her patience, tolerance and understanding during the time we have spent together in the laboratory. I have learned a lot from her and took great pleasure to work with her which made this study much more pleasant.

I would also like to thank Koray Yeşiladalı for his priceless help and for his guidance through the department of Molecular Biology and Genetics. I am also indebted to Esra Yüca and the team of the fungi laboratory for sharing thoughtfully their molecular biology knowledge and experience with me.

I would like to thank Vefa Ezirmik who has conducted Optical Profilometer analysis of aluminum specimens and encouraged me constantly.

I would like to thank to the Metallurgical and Materials and Molecular Biology and Genetics Departments of Istanbul Technical University for the encouragement and the support they have provided along my studies.

I would like to thank my friends, for their motivation, moral and technical support in every step of my research and while I was writing this thesis.

I also would like to mention that this study is supported by Turkish State Planning Organization.

At last, but not least, my deepest thanks belong to my family, first, my parents for their endless support, my aunt, Prof. Dr. Betül Kırdar for kindly guiding me towards science and all the other members of my closest entourage for providing me with the strength, motivation, confidence and moral to do my best in my education and career.

May, 2007 Zehra Beril Akıncı

TABLE OF CONTENTS

ABBREVIATIONS

AAO	**:** Anodic Aluminum Oxide
AFM	**:** Atomic Force Microscopy
APS	**:** Ammonium Per Sulfate
DR	**:** *Deinococcus Radiodurans*
EBL	**:** Electron Beam Lithography
EUVL	**:** Extreme Ultraviolet Lithography
FIB	**:** Focused Ion Beam
HPI	**:** Hexagonnaly Packed Intermediate
NIL	**:** Nano-Imprint Lithography
PMMA	**:** Polymethyl methacrylate
SDS	**:** Sodium Dodecyl Sulfate
SDS-PAGE	**:** Sodium Dodecyl Sulfate Polyacrylamide Gel Electrophoresis
TEMED	**:** Tetramethylethylenediamine
UV-NIL	**:** Ultraviolet Nano-Imprint Lithography

INDEX OF TABLES

Page

INDEX OF FIGURES

Page

İNORGANİK YÜZEYLERDE HÜCRE DUVAR PROTEİNLERİ İLE ORGANİK NANOYAPILARIN OLUŞTURULMASI

ÖZET

Nanoteknoloji sadece yeni özelliklere sahip yüzeylerin oluşturulmasında değil aynı zamanda daha düşük maliyetle daha hızlı çalışan yeni aletlerin yaratılmasında da önemli bir role sahiptir. Bu yeni yapıların geleneksel olanlara oranla daha üstün opto-elektronik, manyetik veya katalitik özellikleri vardır.

Moleküler düzeyde üretim gibi birçok önemli teknolojik uygulamaya nano boyutta yapılandırılmış yüzeylerle ulaşılabilmektedir. Bu yüzeyler beklenenden farklı fiziksel ve kimyasal özelliklere sahiptirler. Bu amaçla nanometre seviyesinde malzeme üretimini kontrol edebilmek için en kritik teknolojik sorun ise yüzeylerin bu boyutlara kadar yapılandırılmasıdır. Her ne kadar elektron demeti litografisi, taramalı prob litografisi ve odaklanmış iyon demeti litografisi gibi nano-litografi teknikleri 100nm'nin altında boyut ve mesafelerde çalışmak üzere geliştirilmiş olsa da bu tekniklerin yüksek maliyeti ve düşük üretim hızları halen sorun oluşturmaktadır.

Bu nedenle, alternatif nano üretim metotları aramak için son on yılda doğadaki örneklerden esinlenilmeye başlanmıştır. Nanoteknolojik uygulamaların büyük bir bölümü kendi kendine birleşen, özellikle de belirli şekillere sahip olan yeni, gelişmiş yüzeylere ihtiyaç duymaktadır. Bunun gerçekleştirilebilmesi için nano-biyoteknoloji bilimi doğada evrim süreci boyunca kendiliğinden ortaya çıkmış olan, son derece kompleks nano yapılardan ilham alma yolunda gelişmiştir.

Moleküler düzeyde kendi kendine birleşmenin bir nano sentezleme stratejisi olarak kullanılmasında temel prensip şekillendirici moleküllerin ve supramoleküler birimlerin oluşturulmak istenen yapıya doğru şekilsel bütünlüğü sağlamak için otonom hareket etmeleridir. Bu olayın birçok avantajı vardır. İlk olarak nano boyutta üretimin en zor bölümünü teşkil eden, yapıların atomik düzeyde şekillendirilebilmesi sorunu, kendiliğinden gerçekleşerek çözülmüş olur. İkinci bir avantajı, karmaşık ve kullanışlı yapıların biyolojiden ilham alarak oluşturulmasıdır. Üçüncü olarak, biyolojik yapıları ortaya çıkan son ürünün bir parçası olarak kullanmasıdır. Son olarak, sistem termodinamik kurallara uygun olarak işlediğinden sonuçta elde edilen malzemeler ya çok az hata içerir yada kendi kendini onarabilme özelliğine sahiptir.

Bu çalışmanın amacı, nano boyutta yapılandırılmış malzemeleri "bottom-up" üretim stratejileri ile üretmektir. Hücre duvarı proteinlerinin özellikle dikkat çekici olmasının nedeni, kesin belirlenmiş aralıklarla, iki boyutlu kristal dizileri kendi kendilerine çok çeşitli fiziko-kimyasal koşullar altında oluşturabilmeleridir. Hücre duvar proteinleri bir çok bakteri ve arkea'nın hücre duvarının yüzeyinin en üst kısmında bulunurlar. Protein monomerleri veya glikoprotin serilerinden oluşurlar. Moleküler ağırlıkları 40 ila 200kDa arasındadır. En ilgi çekici özellikleri 3-30nm arası latis aralıklarıyla düzenli yüzey yapıları oluşturmaları ve *in vitro* veya *in vivo* ortamlarda kendiliklerinden organize olarak oblik (p1,p2), kare (p4) ve altıgen (p3,p6) diziler

oluşturabilmeleridir. Bu dizilerin kalınlıkları 5 ila 10nm arasında olup, ortalarında bulunan delikler 2-8nm arasında ve boyutsal ve morfolojik olarak benzerdir.

Bu çalışmada, *D. radiodurans* bakterisinden saflaştırılan hücre duvar proteinleri kullanılmıştır. Bu proteinler altıgen simetriye sahiptir ve 18nm latis aralıkları vardır. Merkez bölgesi altı adet aynı protein monomerinin bir boşluk bölgesini çevrelemesinden oluşur.

Saflaştırılan hücre duvar proteinleri kullanılarak üç farklı malzeme üzerinde oluşturulan nano boyutlu yapıların incelenmesinde ve görüntülenmesinde atomik kuvvet mikroskobu kullanılmıştır. Ön deneylerde silikon ve mika malzemeleri ile çalışılmıştır. Bunun nedeni bu iki malzemenin oldukça temiz ve çok düz yüzeylere sahip olmalarıdır. Buna karşılık alüminyum örneklerin yüzeylerinin çok dikkatli bir şekilde elektrolitik olarak parlatılması ve yüzey pürüzlülüğünün düşürülerek proteinlerin kristallenebilmelerine olanak veren uygun yüzeyler elde edilmesi sağlanmıştır. İlk çalışmalardan elde edilen sonuçlar hücre duvar proteinlerinin düz yüzeylerde kristallenmelerinin oldukça fazla olduğunu göstermiştir. Buna karşılık, tek katmanlı bir kristallenmeden ziyade çok katmanlı yapıların oluştuğu gözlenmiştir. Alüminyum üzerinde, hücre duvar protenleri kullanılar bir nano yapı oluşturulması bu alışmada ilk olarak gösterilmiştir.

Sonuç olarak, nano-biyoteknolojik yaklaşım ile hücre duvar proteinleri, biyolojik moleküllerin nanometer boyutunda yapıların ve nano-şablonların oluşturulmasında kullanımının gelecek çalışmalar için alternatif ve umut vaad edici bir yol olduğu gözlenmiştir. Ayrıca, gelecek çalışmalarda protein temelli yapıların genetik değişiklikler ile nano boyutlu şablon ve dizilerin daha fonksiyonel özellikler kazanmasında kullanılabileceği düşünülmektedir.

NANOTEMPLATE FORMATION ON INORGANIC SUBSTRATES BY USING SURFACE LAYER PROTEINS

SUMMARY

Nanotechnology not only can produce surfaces with novel functionality, but also new devices that are cheaper and faster than conventional ones, and which may have other advantages such as unique optoelectronic, magnetic, or catalytic properties that can be tuned by varying the size and/or the interparticle spacing of its constituents.

Many important technological applications such as molecular level manufacturing of systems can be attributed to nanostructured surfaces because they exhibit unique physical and chemical properties. One of the crucial technological challenges, however, is the development of effective patterning methods to control assembly on a nanometer scale. Although nanolithography techniques such as electron beam lithography (EBL), scanning probe lithography (SPL), and focused ion beam lithography (FIBL) permit the creation of ordered nanostructured arrays with high resolution (i.e., 100 nm features and/or spacings) and very good control over particle shape and spacing, the cost of these techniques is high and the fabrication process is relatively slow.

Therefore, looking into nature for an alternative parallel approach for nanofabrication has inevitably emerged in the last decade. A great number of nanotechnological applications require the development of sophisticated self-assembled surface substrates, particularly those with defined spacing. For this to be achieved, the promising science of nanobiotechnology take inspiration from the nature which through evolution has produced extremely complex nanostructures via self-assembly method.

The basic principle of molecular self assembly as a nanofabrication strategy is that it brings together designing molecules and supramolecular units in a way that they aggregate into desired structures via shape-complementarity. The advantages of this phenomena are numerous. First, it makes naturally happen the most demanding task of nanofabrication which is atomic level modification of structures. Second, it takes inspiration from biology and realizes the development of complex, functional structures. Third, it utilizes biological entities directly as a part of the final systems. Finally since it functions by thermodynamic rules, the results is structures that are relatively defect free and self healed.

The aim of this study was creating nanostructured materials based on bottom-up manufacturing strategies. Of particular interest are surface layer proteins (S-layer) which self-assemble on the surfaces as biological scaffolds. S-layer proteins are of great importance in bionanofabrication since they self-assemble into well defined two dimensional crystalline arrays on a wide range of topological and physico-chemical environments. S-layer protein lattices are found on the outermost surface of many prokaryotic microorganisms (i.e., bacterial and archaea) and are composed of protein

(or glycoprotein) monomers with a molecular weight of 40-200 kDa depending on the,particular microbial species. S-layers are particularly interesting since they display a highly repetitive surface structure with nanometric lattice spacing (3-30 nm) and possess the useful ability to self-organize (either in vivo or in vitro) to form oblique (p1, p2), square (p4) or hexagonal (p3, p6) array structures only 5-10 nm in thickness. Pores of identical size and morphology in the size range of 2-8 nm are typically found.

The *D. radiodurans* S-layer, utilized herein also known as the hexagonally packed intermediate (HPI) layer, has a p6 rotational symmetry with a reported spacing of 18 nm37 between each protein core region. The core region itself consists of six identical protein monomers enclosing a single central pore, and is in turn surrounded by six vertex regions of identical size.

Atomic force microscopy has been used to investigate nanostructures formed by s-layers on three different substrates. In the preliminary experiments, silicon wafer and mica are used as control substrates since they exhibit a relatively clean and extremely flat surface topographies. However aluminum samples had to be electropolished very carefully in order to allow the crystallization procedure on the surface. Results of the initial studies showed that S-layer recrystallization was very abundant on the flat surfaces. However the control over the monolayer formation was not possible and many multilayered crystallization was observed. In this study, generating a nanomask on aluminum surface via S-layer proteins was demonstrated for the first time.

In conclusion, from a nanobiotechnological standpoint surface layer proteins offer an alternative promising way of using biological molecules for nanometer scale synthesis of nanotemplates or nanomasks. Moreover as a future vision protein-based scaffolds can be genetically modified which will potentially improve their nanoarray fabrication properties.

1. INTRODUCTION

The hybrid area between biology and materials science which involves the processing, fabrication and packaging of organic or biomaterial devices or assemblies in which the dimension of at least one functional component lies between 1 and 100nm is called “bionanotechnology”. This research area is characterized by its highly interdisciplinary nature and features a close collaboration between life scientists, physical scientists, and engineers. The emerging field of supramolecular architectures requires an integrated exploitation of biological principles, physical laws (quantum effects), chemical properties and cognitive sciences. Imitating nature’s way to redesign or to develop conventional technologies of material science is a new approach for engineering nanostructures. Hence surface science which is a major part of the materials science becomes the frontier between biological interactions and material specifications in order to generate designed templates for further applications [1].

There are several techniques for generating a nanotemplate on different surfaces. Any of these methods has its advantages as well as its drawbacks. Among them, lithography is the most widely used nanotemplating technology. In general terms, lithography consists of the transfer of a pattern onto a substrate via a photoresist mask by using light. Traditional lithography techniques are developed for micro electronics industry and revealed to be insufficient for nano-scale fabrication. Limitations of size and shape controlled features in conventional lithography techniques, long processing times, high cost of modern lithography techniques and restricted pattern geometries in soft-lithography made clearly seen the need for new approaches for engineering surfaces at nano-scale. Thus, photolithography will eventually be unable to scale down further and may have to be abandoned. Researchers are currently looking into better lithography-based techniques (with wavelengths further into the non-visible spectrum) to use the infrastructure in place. However, it is likely that industry will look beyond lithography in the distant future [2]. A promising approach is using the “bottom-up” philosophy, in which molecular components “self-assemble” into larger structures.

Self-assembly is the essential principle which produces and guides structural organization on all scales. Self-assembly of molecules arranging every single molecule or atom one at a time is due to the chemical complementarity and structural compatibility of the atoms and molecules both present weak hydrogen bonds or covalent bonding interactions that bind building blocks together in the fabrication process. The logic of the self-assembly is that molecules will always seek the lowest energy level available to them, whether this means bonding with an adjacent molecule or reorienting physical positions.

Biological self-assembly has emerged over times a hybrid methodology that combines nature's molecular tools with synthetic nano-scale constructs [3]. The process is called biopatterning, a concept for depositing active biomolecules on solid surfaces with nano-scale spatial resolution and via this pattern generating self-assembly of inorganic constructs on conventional substrates. This method of nanofabrication has been shown to be a robust strategy to construct functional nanopatterns [4].

Several biomolecules such as proteins which are promising molecules due to their binding and self-assembly characteristics or lipozomes could be used for biopatterning processes. Among them, bacterial surface layers (S-layers) have been shown to function as versatile substrates for high precision self-assembly of molecules, metals and semiconductors. S-layers are 2D proteins that make up the outermost cell covering of bacteria. S-layer proteins have the intrinsic property to reassemble into two-dimensional arrays on surfaces of a broad spectrum of materials (e.g. silicon wafers, metals, polymers) and interfaces (e.g. planar lipid films or liposomes), the arrangement of functional domains on each S-layer unit cell is repeated with the periodicity of the S-layer lattice at a distance of approximately 10 nm, enabling the formation of regular arrays of bound molecules and particles. They have high density functional groups in definite locations and orientations hence by using bio-patterning, the biomolecules can be controlled spatially to form ordered lateral arrays ranging from the nano-scale to the micro-scale [5].

In this present study, surface layer proteins of deinococcus *radiodurans* were used to biopattern inorganic surfaces and obtain functional nanotemplates. Nanopattern formation experiments were performed on three different substrates: silicon wafer, mica and aluminum respectively. Characterization of these organic-inorganic hybrid

structures has been realized by atomic force microscopy (AFM). The biopatterning capabilities of s-layer proteins were first tested using silicon wafer and mica because of the easiness of both to prepare as fresh, clean and flat surfaces, and consequently the proteins can be conveniently visualized via AFM. Next, self assembly of s-layer proteins on aluminum surface were investigated in detail for potential use of aluminum nanotemplates in nanobiotechnological applications.

As explained before, conventional technologies (like lithography) have limitations to obtain aluminum templates with an accurate geometry in nano-scale. The aim of this study is to demonstrate the formation of aluminum nanotemplates using s-layer proteins as an alternative technique to conventional nanotemplating technologies. For this purpose, surface treatment of aluminum is required because s-layer proteins are not strongly adsorbed on corrugated surfaces. As a powerful tool for surface treatment, electropolishing was utilized to decrease the surface roughness of aluminum.

In order to obtain s-layer proteins, the strain *Deinococcus radiodurans* was chosen due to its ease of production and abundance of its s-layer proteins. Since the S-layers of D.*radiodurans* have p6 lattice symmetry they are also called hexagonally packed intermediate (HPI) layer proteins [5]. The so-called HPI layer represent the major cell envelope protein of the radiotolerant bacterium *Deinococcus radiodurans,* is thoroughly associated with the outer membraneous layer (‘backing layer’) of the bacterium and covers its surface completely [6].

Results indicate that s-layer proteins form a definite pattern on the surfaces allowing further processing of substrates. Here, we demonstrated that aluminum nanotemplates can be generated by using S-layer proteins for the first time as an alternative method to conventional nanotemplating technologies

2. BACKGROUND INFORMATION

2.1. Nanotemplates

2.1.1. Importance of Nanopatterned Surfaces

The growing need for the fabrication of nano-devices, such as nano-electronics, nano-optoelectronics or nano-sensors brought the necessity of acquiring new surface nanopatterns on technologically important substrates. The construction of new devices using bottom-up approaches require precisely positioned molecules or particles on a desired geometry. Therefore developing new engineered surface patterning methods is the new challenge in the nano-fabrication field.

At nano-scale level, materials exhibit unique characteristics based on physical phenomena, hence the physical and chemical rules which are valid in the macro-scale materials might not reflect their displayed properties. Theoretical predictions in molecular and nanometer-scale structures such as organized quantum dots, and electrical transport in nanotubes and nanowires have been recently confirmed by experimental research which is realized in the field of nanometer-scale electronics and photonics. Moreover, the small size of colloidal particles of metals, functional ceramics and semiconductors allow the potential use of those materials with electronic, optoelectronic and magnetic properties that derive from their small size. Their application as chemical, biological, and optical sensors, spectroscopic enhancers, nanoelectronics, and quantum structures, among others derive also from these properties. Therefore a successful integration of nano-scale materials to technology requires creation of millions of these structures in parallel either by existing or new patterning techniques [7].

Those patterning techniques should be applicable for a wide range of materials and should be able to create different features with controllable shape, size and spacing. There are numerous nano-patterning methods to generate nanostructure arrays on substrates. Basically they are lithographic methods (such as electron-beam, ion-beam, extreme ultraviolet and X-ray, nano-imprint lithography), self-assembly processes, scanning probe techniques, and methods that utilize diblock-copolymers.

nanometer-scale processing which becomes more and more demanding. It is essential for sustaining the emerging needs of the nanotechnology to develop new reliable surface nano-templates with high performance and low equipment cost [8].

The nano-patterns realised on surfaces allows the precise control of the manipulation and the placement of individual atoms and to foresee their nano-scale arrangement, performance and properties [9].

2.1.2. Template Directed Fabrication of Nanostructures

Over the past decade, nanotechnology has turned towards the junction of nano-electronics, nano-photonics, nano-electro-mechanical-systems (NEMS), and other components into single "intelligent" devices. However, despite significant development in nanostructure synthesis and nanodevice fabrication, there remain considerable difficulties in realizing such devices, primarily due to the lack of ability to control nano-sized components to these devices.

As the fabrication of more and more complex nano-devices is needed, the control mechanism over the precise location and shape of those structures passes through creating a desired template on a given substrate. Conventional approaches to synthesis of nano-scale materials are generally energy inefficient, require stringent synthesis conditions, and often produce toxic byproducts. Moreover they still use "top-down" approaches, and even the most advanced microtechnology and recently developed nanotechnology, such as self-assembly through chemistry, nano lithography, and micro-contact printing, necessitate considerable external operation that curtail the achievement of complex 3D architectures and robust scale-up, and, for this reason, limit the potential [7].

To generate nano-patterns in order to produce nanostructure arrays, numerous methods have been developed. Basically those are lithographic methods (e.g. electron beam, ion beam and x-ray lithography), scanning probe techniques, diblock-copolymers and self-assembly processes.

Lithography has been the most widely used method for micro-production due to its precise control over the size, shape and spacing properties. There are several lithography techniques such as photolithography, x-ray lithography, focused ion beam lithography, nano-imprint lithography, interference lithography or scanning

probe lithography. Among them the most widespread technique for nano-scale manufacturing is electron beam lithography.

Secondly, self-assembly processes seem to produce promising results for manufacturing large areas of nano particle arrays. The self -assembly method is based on molecular interactions and have drawn attention when the top-down approaches of conventional lithography techniques revealed to be insufficient for the emerging needs of nanofabrication.

The third technique for writing or creating patterns on substrates is the scanning probe microscopy (SPM). SPM uses both the tips of scanning tunneling microscopy (STM) and atomic force microscopy (AFM) to modify, by physical or chemical ways, the surface of technologically important substrates. Moreover SPM techniques offer a great range of resolution quality going from the micrometer to nanometer scale.

The diblock-copolymer method offers a promising approach to create nanometer scale patterns. Block copolymers are constituted of two or more different chains of polymers chemically bound to each other. Their ability to self-assemble in densely packed arrays makes them extremely interesting molecules for the generation of nano-structures . The polymer serves to achieve an ordered porous nano-structure on the surface which can be used as a nano mask to fabricate nano-dots or nano-pores. Furthermore when combined with conventional lithography techniques block copolymers have the advantage to offer high resolution and process control.

Another approach for the template directed synthesis of nanomaterials is using anodic aluminum oxide templates [48]. Since nanostructure formation by self-organizing methods have attired attention among them, the anodic aluminum oxide (AAO) templates have been considerably exploited in synthetic nanostructure material due to their advanteages such as controllable pore diameter, periodicity of the pores and extremely narrow distribution of pore size.

Unfortunately all these methods have some drawbacks and restrictions. For instance limited pattern area, low throughput, long process time and high cost are the main limitations of the electron beam lithography (EBL) method.In self-assembly process and in diblock copolymer approach it is difficult to control spatial size and distribution of nano structures and the substrate material choices are relatively few.

Also, the surface cleaning is hard to obtain due to the effect of by-products occurred in the preparation process of self-assembly particles. The SPM techniques are slow and not capable of generating large areas of patterned structures on the surfaces. Moreover, the currently available alumina templates are limited to planar geometry. This restricts the pore growth to a single direction, limiting the integration possibilities for electronic applications.

In summary, the production of the full potential of nano-technological systems has so far been restricted because of the difficulties in their controlled-synthesis and the successive assembly into useful functional structures and devices [7]. All micro and nanofabrication techniques used today have more or less some restrictions. These restrictions makes inevitable and only a time issue the invention of new processes. Thus, in order to obtain highly ordered nano structures with high throughput, low cost and high control over the size, shape and the spacing of nano-particles, new methods have to be developed and optimized. Therefore to solve the problem of controlled miniaturization and to manage molecules at the atomistic scale are the challenges in nano-technology and nano-fabrication [10].

2.2. Nano-patterning Technologies

Lithography is the general name for many patterning technologies. The conventional lithography techniques has been developed for the semiconductor industry and micro-fabrication. Optical lithography, also well known as ‘photolithography’, has leaded the manufacturing and the scaling down of the feature sizes of integrated circuits, allowing the outrageous growth of the semiconductor industry

in the semiconductor industry The process involves the transfer of a pattern via a photosensitive polymer-based material which is coated on the substrate (usually Si) by the exposure to a radiation source. The photosensitive material acts as a mask and as a result the properties of exposed areas are different from the unexposed ones [11]. The basic steps o a photolithographic process are given in the figure 2.1.

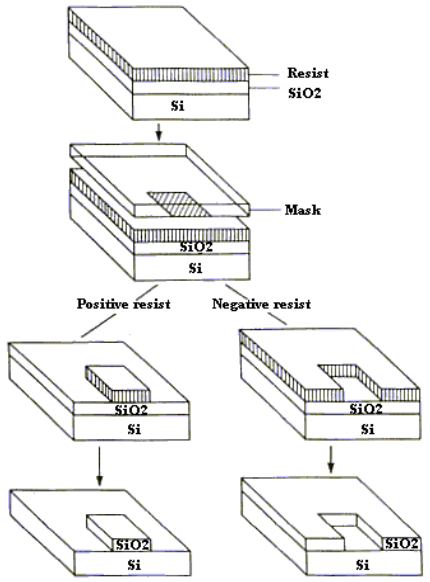

Figure 2.1: Example stages of photolithography [11]

However this method has also some drawbacks which limit its resolution. Optical lithography is appropriate for feature sizes beyond 100nm and 70nm with the use of respectively 193nm wavelength and 157nm wavelength tools yet the reduction of feature sizes down to 50nm and below will require improved kinds of lithographic procedures. Hence to cover the needs of nano-fabrication more advanced lithography tools are in use today [3].

The theoretical limitations of the printed feature using photolithography come from the Rayleigh scaling equation:

$$F = k \cdot \frac{\lambda}{N_A} \tag{2.1}$$

Where; F is the minimum line width of the printed feature, k is the dimensionless scaling factor and typically equals 0.5, λ is the exposure wavelength and NA is the numerical aperture.

Most attention has been focused on reducing the wavelength, as it scales proportionally to the resolution limit. Lasers used in the industry have included the use of KrF (~250 nm) laser, ArF (~190 nm) laser, to the current use of F_2 laser, which has a wavelength of 158 nm. In order to improve the resolution limits of

photolithography, industry has also looked into increasing numerical aperture. However, increasing numerical aperture decreases depth of focus (DOF), the vertical length in which the image can be focused, according to the Rayleigh scaling.

$$D_F = 0.6 \cdot \frac{\lambda}{{N_A}^2} \tag{2.2}$$

Where, D_F is the Depth of Focus, 0.6 is the dimensionless factor which depends on imaging details, λ is the exposure wavelength and NA is the numerical aperture. Current state-of-the-art photolithography tools use deep ultraviolet (DUV) light with wavelengths of 248 and 193 nm, which allow minimum feature sizes down to 50 nm [12]

Although several studies were focused to improve photolithography it is likely that alternative approaches beyond photolithography are needed.to generate nano-structures. Some of the most recent techniques are electron beam lithography, ion beam lithography, x-ray lithography and scanning probe lithography [13].

Electron beam lithography (EBL) is derived from the early scanning electron microscopes in late 1960's. The primary advantage of this technique is that it overcomes the diffraction limit of light and makes features in the sub-micrometer regime. It uses a focused beam of electrons to generate a desired pattern on the wafer whereas optical lithography uses light for the same purpose. The basic working principle involves the formation of an electric field between a cathode and an anode. The electrons emitted from the cathode which have also the function to focus them into a beam, are accelerated towards the anode where they pass through and hit the specimen's surface.

The surface of the specimen is covered with a resist film sensitive to electrons which are used to directly etch onto it. The resists are generally polymers dissolved in a liquid solvent and are layered to the substrate by the spin coating method. The primary advantage of this technique over the optical lithography is its greater patterning resolution obtained by e-beam lithography due to the shorter wavelengths (10-5keV) of electrons. However the resolution of an electron beam lithography system can be affected by electron scattering and also longer process times and high cost of the equipment are the main disadvantages.

One other advanced lithography method is X-ray lithography (XRL). The diffraction limit problems of optical lithography are resolved with the shorter wavelengths (0.01 to 1 nm) of X-rays. High resolution imaging at 100 nm scale and below by XRL is possible as a result of this small wavelength. X-rays can be produced by several methods such as electron bombardment, plasma X-ray sources, and synchrotron radiation. X-rays occurs when the electromagnetic radiation of the high-energy electrons strike matters. In addition, X-rays generate secondary electrons as in the cases of extreme ultraviolet lithography and electron beam lithography.

An X-ray transparent membrane material with a pattern on it is used as mask which is composed of gold, tantalum or tungsten. The mask is exposed to a parallel beam of x-rays. Consequently the resolution of the pattern is limited to the variations of the mask. Moreover the costs of X-ray masks are higher than optical lithography masks due to fabrication complexity [14].

Another nano-lithography method is focused ion beam (FIB) lithography which is a variation of electron beam lithography technique where a focused ion beam is used instead of an electron beam. In this method, an ion beam, controlled by a computer scans across the substrate surface and act on an electron sensitive coating. The pattern data is transferred to the controlling computer, which then directs the electron beam as to realize the pattern on the substrate pixel by pixel. One advantage of this method over EBL is the possible *in situ* doping of ions or possible *in situ* material removal by ion beam etching. However, FIB is a slower process and it should not be expected to afford the requirements of mass production of nano-devices [15].

Extreme ultraviolet lithography (EUVL) is a technique which shows many similarities with conventional optical lithography such as the system configuration. The EUVL system is composed of an EUV source, illumination optics (condenser optics), imaging optics, and a reflection mask. However it has also some important differences from conventional lithography and most of them are due to the use of 13.5 nm wavelength. EUV light of this wavelength is generated by creating a hot plasma of a target material (e.g. Xe, Sn, or Li) which can be excited in two ways, either by excitement via a high power laser in laser produced plasma (LPP) sources or by an electrical discharge in discharge produced plasma source. Besides, since all matter absorbs EUV radiation, the EUV lithography needs to take place in a vacuum [16].

Nano imprint lithography is a promising way to print nanometer-scale geometries in a relatively simple way with a low cost while the conventional methods have some major drawbacks (e.g. high prices for EUVL, no source with sufficient output) in these areas. There are many different types of Nanoimprint Lithography, the two most important ones are: Thermoplastic Nanoimprint lithography and Photo Nanoimprint Lithography

The first one is also known as thermal imprinting. A polymer is heated to temperatures higher than its glass transition temperature (T_g) above which the polymer is liquid and a mold is pressed on it. Once the polymer is cooled down the surface is textured in the mold's shape. The most used polymer is PMMA (poly-methyl methacrylate) of which T_g is higher than 110^{o}C This method requires high temperatures and the pressure needed is between 40 and 130atm.

The second technique is a variation of thermal nano imprinting and is called photo nanoimprint lithography. It functions by bringing in contact a transparent template with a monomer, causing it to spread across the surface and fill the pre-decided structures of the template. Ultraviolet light photo-polymerizes the monomer and when the template is separated from the wafer it leaves a copy of the template on the substrate surface. This method is also called ultraviolet nano imprint lithography (UV-NIL). The advantage of UV- NIL is that it functions at room temperature and at low pressures and it has the ability to create patterns sub 10 nm features [17,18].

As the needs of the nanotechnology become more and more demanding every day new tools to manufacture surfaces even more precisely are required to be developed. Scanning probe microscopes are not anymore only a tool for observing the surface structure but also to shape them at nano-scale features. AFM based lithography techniques are simple and permits to control easily the structure and precise location of the features on various surfaces.

Scanning probe microscope lithography uses the tip for scribing and indenting by physical means. The surface itself is very often damaged when the force is applied to the surface for imaging the surface topography is too big. This problem has been the inspiration of SPM lithography. Applied patterns can be obtained on the surface by controlling the tip movement and increasing sufficiently the magnitude of the force. For further applications SPM can modify the surface by physical or chemical means

depending on the nano-scale probe. On the other hand, SPM lithography has to encounter still several problems such low throughput, reproducibility and extensive processing time before being commercialized properly [19].

Another approach to produce nanometer scale well defined surfaces is to use soft lithography techniques such as block co-polymers as lithographic masks. Soft Lithography is the general term for a set of techniques that rely on printing and molding to make microstructures and nanostructures. It is called "soft" due to the use of elastomeric materials. Soft lithography constructs features at the nanometer scale and was originally developed in order to circumvent the limitations of photolithography, which has been the basic technology used for making all microelectronic systems. include the technologies of Micro Contact Printing, replica molding, microtransfer molding, micromolding in capillaries and solvent-assisted micromolding are techniques included in soft lithography. Among them, block co-polymers consists of two (called diblock co-polymers, the most basic type) or more polymer chains chemically bound to each other. It is known that block co-polymers self-assemble onto surfaces in three dimensional structures by thermodynamical means because of the microphase separation [20]. The basic principle of the first phase for any Soft Lithographic technique is the formation of a master via proven techniques, such as photolithography, e-beam, or micro-machining it could also be an existing structure that does not require processing like a human hair or some woven fabric. An elastomer, such as polyurethane or a silicone, is poured onto this surface, hardened using heat or ultraviolet light, and peeled off to yield a ‘mold’. The resulting mold is the exact structural inverse of the original surface - down to nanometer accuracy depending on the combination of materials used and the precision of the replication process. The deformation of the stamp through pairing or sagging is unavoidable and shortens the durability of stamp itself. In addition, the spreading of fluidic printing ink wetted on stamp during micro-contact or micro-transfer process is another inevitable problem. These problems make it difficult to achieve an accurate and well-defined pattern using soft lithography. [11,21].

Over the past decade, nanometer-scale assemblies have been realized by mimicking the nature’s self-assembly procedure. Nano-scale architectures can be constructed via self-assembly of naturally occurring or designed molecules. Some examples are molecular recognition-directed molecular assemblies, surfactant bilayer membranes,

Langmuir-Blodgett films, self-assembled monolayers and alternatively deposited polyelectrolyte multi-layers.

Among them surfactant bilayers are inspired directly from biomembranes. The Langmuir-Blodgett (LB) technique is one of the most conventional methods of nano-film fabrication. The polyion complex technique was proposed to immobilize water-soluble bilayer forming amphiphiles and counter-charged polymers as polymeric LB films [22].

To sum up, it would not be wrong to say that lithography has limits for the possible smallest feature size hence it may never be possible to fabricate nano structures directly by lithography. Soon or later lithographic techniques will reach their fundamental limits in order to cover up the needs of nano industries. While the top-down approach uses the conventional tools of several lithography techniques, the bottom up approach consist of designing materials via molecular interactions and self-assembly. The limits of conventional methods such as high operating costs, multiple-step processes and restricted material choices leaded the lithography industry to turn on to bottom-up methods. New methods like nano-imprint lithography, AFM based lithography, block co-polymer based lithography or self assembled monolayers come out to be more promising alternatives by any means in nano-scale patterning and fabrication but yet they are not completely effective methods and the search of alternatives beyond these techniques is still going on.

2.3. Surface Layer Proteins

2.3.1. Historical Outline

As they have to live in very competitive habitats most bacteria and archaea has developed a supramolecular cell-wall structure. S-layer proteins, described for the first time by Houwink as “macromolecular monolayer” in the cell wall of *Spirillum* sp. at 1953 constitutes the outermost component of this structure. Succeeding the discovery of Houwink, a relatively long time period has been needed before the complete understanding of the implications of this cell wall structure.

Crystalline surface layers are found in many bacteria and they form a universal feature in almost all archaea. A large number of bacterial strains possess different forms of this layer.

S-layer research have a history of nearly three decades. During this time period a great variety of names have been attributed to these molecules. Historically given some of these names are:

- Tetragonal layer (Aebi, 1973)
- Regular surface layer (Beveridge and Murray, 1974)
- S-layers in gram positive and gram negative strains (Sleytr, 1978)
- Additional layer (Udey and Freyer, 1978)
- Hexagonally packed intermediate layer (HPI) in *Deinococcus radiodurans* (Baumeister and Kübler, 1978)
- Middle and outer wall protein in *Brevibacillus brevis* (Yamada et al, 1981)
- Cell surface glycoprotein in *Halobacterium halobium* (Lechner and Sumper, 1987)
- Surface array protein in *Campylobacter fetus* (Blaser and Gotschlich, 1990)"

Murray described hexagonally packed subunits in Micrococcus R. and Spirillum sp. in 1960's but the "S-layer" term which defines two dimensional crystalline arrays of proteinaceous subunits that form surface layers on prokaryotic cells was agreed on at the second international workshop of S-layers (Vienna) in 1987. (Sleytr et al.).

Following this time period, several investigations have been focused on imaging of s-layers using electron microscopy. Among various methods of preparation techniques such as metal shadowing, negative staining, freeze-drying and freeze etching, ultra thin sectioning , freeze etching preparations realized by Sleytr et al. in late 70's gave strong evidence about the dynamic self-assembly process of s-layers on growing cells. The electron microscopy studies showed that s-layer subunits may posses various symmetries: linear (p1,p2), tetragonal (p4) and hexagonal. (p3,p6) as illustrated in the figure 2 [23].

2.3.2. Occurrence and Structure

Almost 30 years of research have proved that S-layers are one of the most commonly observed bacterial cell surface structures [24]. As they have to live in very competitive habitats most Bacteria and Archaea have developed a supramolecular cell-wall structure and S-layer proteins constitute the outermost component of this

structure. It is now an accepted fact that S-layers evolved together with prokaryotic envelopes even so they show many variations in their structure and chemistry. Some archaea have an S-layer which is strongly connected to the plasma membrane and make it a part of the bilayer. In gram positive bacteria and in archaea S -layer happens to be on the surface of the cell matrix. In gram negative bacteria the S-layer is a part of the lipopolysaccharide (LPS) component of the outer membrane. Moreover S-layer lattices can be constituted from more than one species and, each of which is composed of different subunits [24-26].

S-layers are the most basic kind of biological membrane in morphological, chemical and morphogenetic terms. They are composed of single protein or of glycoprotein species. S-layers are classified to several groups based on their space groups, unit cell size and arrangement of pores [27]. S-layer lattices show oblique (p1, p2), square (p4) or hexagonal (p6) symmetry. However hexagonal symmetry is dominant among Archaea. The symmetry means that one morphological S-layer unit is formed by a one, two, three, four or six identical glycoprotein subunits. P2 lattices that show the finest lattice constants (2 to 3nm), medium lattice constants from 6 to 12nm are present in p2, p4 and p6 symmetries and large lattice constants, in the order of 13 to 23nm, are observed in p4 and p6 symmetries. Figure 2.3 represents a computer reconstructed image of different S-layer lattices [25].

The subunits have a center to center spacing in the order of 2.5 to 35nm and their molecular mass is in the range of 40 to 200kda. The unit cell dimensions are approximately 3 to 30nm. The thickness is 5 to 10nm. S-layer meshwork is highly porous due to the mono molecular assembly structure. The percentage of porosity revealed to be up to 30-70%. The pores are uniform in size and morphology. The size of the pores varies between 2 to 8nm. Often, two or more distinct classes of pores can be found in one S-layer lattice. In most S-layer proteins 40% of the amino acids are organized as β -sheet and about 20% occur as α -helix. They have a high amount of glutamic and aspartic acid (together approximately 15 mol%) and a few, sulfur-containing amino acids [28].

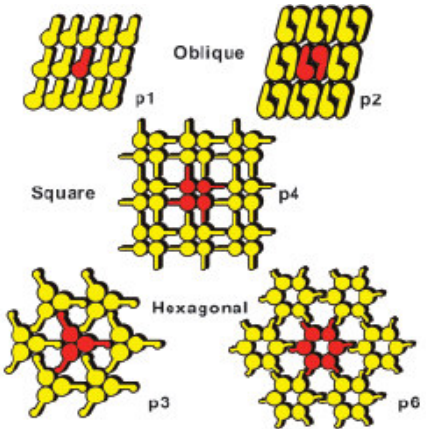

Figure 2.2: S-Layer lattice types, The regular arrays either show oblique (p1, p2), square (p4) or hexagonal (p3, p6) lattice symmetry. The morphological units are composed of one (p1), two (p2), three (p3), four (p4) or six (p6) identical subunits [29]

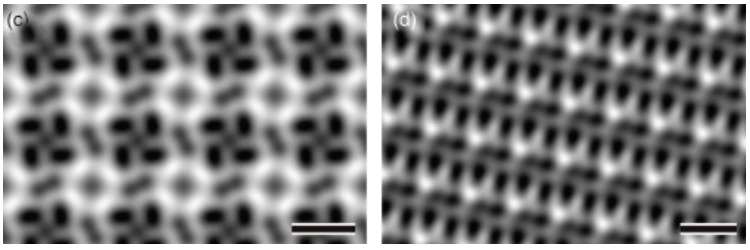

Figure 2.3: Computer image reconstruction of scanning force microscopic images of the topography of the square (p4) S-layer lattice of *B. Sphaericus* (c) and the oblique (p1) S-layer lattice of *Geobacillus stearothermophilus* PV72/p2 (d). Bars: 100nm in (a), 10nm in (c) and (d). [29]

S-layer proteins exhibit a significant difference in surface corrugation and chemistry between inner and outer sides. The S-layers of the bacteria expose a smoother outer surface than the inner surface which is much more corrugated [26]. This is basically due to the excess of carboxyl groups which causes a net negative surface charge on the inner face while on the outer face carboxyl groups and amino groups are found in equimolar amounts.

The interaction of S-layers between their subunits and with the supporting envelope layer is a result of ionic bonds including divalent cations or direct interactions of polar groups, hydrogen bond and hydrophilic interactions. S-layers can be disrupted into their constituent subunits by high concentrations of chemical agents that break down hydrogen bonds (e.g. urea, guanidine hydrochloride or detergents, pH<4). Several studies were focused on gram positive bacteria to understand the dynamic self assembly process of S-layers both *in vitro* and *in vivo* [27,28]. Once the

disrupting agent is removed from the surface the monolayer formation starts. Crystal growth occurs at several nucleation points and continues until the boundary lines of different growing crystalline domains meet with each other. The mobility and density of the proteins on the early stages of crystal formation determine the average domain size. Moreover the surface properties of the substrate such as hydrophobicity versus hydrophilicity influence the crystal growth [30].

2.3.3. Functions of S-Layers

S-layers represent the outermost structure of the cell surfaces if there is no other cell surface component such as glycocalyces or capsules. They form a transition barrier between the cell and the outside world.

Given that S-layers are the most spread out cellular protein type in prokaryotes. It is clear that they have been developed as a response to environmental conditions and according to a natural selection criteria. S-layers are considered to be a part of the cell envelope and their function should not be judged as separated supramolecular structures.

Even after 30 years of research on S-layers, their function still remains yet not entirely clarified. Most information available in literature requires further experimental evidence. Moreover it is clear that all S-layers present in different strains of bacteria and Archaea, are not associated with one single general function but rather they have a multifunctional nature.

Table 2.1: Major functions of S-layer proteins on the cell envelope [26]

Functions of S-Layer Proteins	
1.Determination of the cell shape and cell division	
2. Protective coats	**a)** Prevents predation **b)** Phage resistance, **c)** Prevention or promotion of phagocytosis
3. Adhesion sites for exoenzymes	**a)** S-layers function as physicochemical and morphological well -defned matrice, **b)** Masking the net negative charge of the peptidoglycan- containing layer in Bacillaceae
4. Surface recognition and cell adhesion to substrates	**a)** Molecular sieves in the ultrafiltration range **b)** Delineating in Gram-positive bacteria a compartment **c)** Preventing non-specific adsorption of macromolecules
5. Isoporous molecular sieves	
6. Virulence factor in pathogenic organisms	**a)** Important role in invasion and survival within the host, **b)** Specific binding of host molecules **c)** Protective coat against complement killing **d)** Ability to associate with macrophages and to resist the effect of proteases
7. Fine grain mineralization	

S-layers have generally the function of protective coats, molecular sieves for molecules and ion traps in the ultra-filtration range. They can be target structures for cell adhesion (e.g. adhesion site for exo-enzymes) and surface recognition. S-layers act as physicochemical and morphological well defined matrices. They determine the framework of the cell shape and the cell division in Gram-negative Archaea. In addition, since S-layers are present in an important part of pathogenic organisms it

can be expected that they present a virulence factor such as invasion and survival within the host or specific binding capabilities to host molecules [26,30]. The major functions of S-layers are summarized in table 2.1.

2.3.4. Molecular Biology and Assembly of S-Layers

Detailed studies regarding S-layer structures and morphology have been accomplished in a wide range of microorganisms since almost four decades. Because of the difficulty of cloning S-layer genes in a stable and highly expressed form, the information on the genes encoding these proteins is very limited. Although S-layers are an abundant part of secreted proteins very few (about 30) genes have been cloned and sequenced so far [28]. The information about regulation of S-layer protein synthesis, the translocation of S-layer subunits across components of the cell envelope and about the S-protein domains involved in inter- and intra-molecular interactions is still very scarce. To understand S-layer protein and gene organization, a more focused research on bacterial S-layer genes have been done. Yet some areas such as regulatory mechanisms of transport, biosynthesis and the domains which are responsible for intra- and/or intermolecular interactions of layer proteins still remain unclear. Although the two dimensional structure of all S-layers are identical in their amino acids composition vary widely between species.

Only a few sequence identity have been observed in the majority of the S-layer genes sequenced up to now. Thus an analogue evolutionary process of S-layers structures has been accepted more likely than a homologue process. Also, an individual bacterium can express different S-layer genes if environmental conditions are not maintained stable.

The subunits of S-layer lattices form a network both with each other and with the plasma membrane, outer membrane or the peptidoglycan supporting cell envelope layer. The interaction is a result of non-covalent forces such as hydrogen or ionic bonds and hydrophobic or electrostatic forces. Among these interactions hydrophobic ones have an important role due to the high proportion of non-polar amino-acids (40-60%).

Free amino and carboxyl groups of adjacent promoters in S-layer lattices are closely arranged so that they have an effect on the stability of the array via electrostatic interactions. Furthermore disruption and re-crystallization experiments on S-layer

lattices have shown that the monomolecular units are bound more strongly to each other than to the supporting envelope layer.

The presence of specific binding domains on the N-terminal part of the S-layer proteins for secondary cell wall polymers which are covalently linked to the peptidoglycan matrix of the cell wall is the basic requirement for the dynamic re-crystallisation process of the S-layer lattice on the bacterial cell surface in the course of cell growth and cell division.

The most intrinsic property of S-layer proteins is their ability to reassemble in suspension, at air-liquid interface, at solid surfaces, at lipid films and on liposomes as illustrated in the figure 2.4. Those features allow S-layers to be used in a broad range of nanobiotechnological applications. [26,28,30,31]

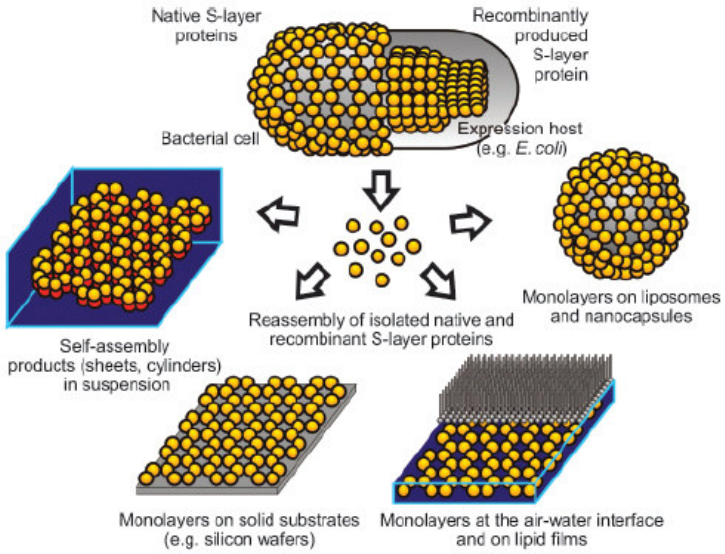

Figure 2.4: Recrystallization procedures of S-layer proteins either in suspension, on solid supports, at the air-water interface,on lipid-membranes or liposomes and nanocapsules [29]

2.3.5. Application of S-layers in Nano and Biotechnology

S-layer proteins possess a wide range of application potential. The most interesting features of S-layers allowing them to be used in nano and biotechnological applications can be cited as:

- Re-crystallization properties of isolated subunits onto solid supports, on air-water interface on Langmuir lipid films and on liposomes.

- Having pores of identical size and morphology at ultrafiltration range
- Well defined position and orientation of functional groups, capable of binding functional molecules with high precision [32].

The use of S-layer proteins as molecular building blocks and patterning tools in a bio-molecular construction kit allows the controlled "bottom-up" approach for engineering functional supra-molecular structures and devices [31].

One important application of S-layers is as ultra-filtration membranes. Possessing pores at identical size and morphology at subnanometer scale with well defined lattice positions is the major advantage of S-layer proteins over conventional polymers which have wide pore sizes and randomly distributed functional groups. Research on the mass distribution and permeability of S-layer revealed that they possess pores of 4 to 5nm allowing them to be used as isoporous molecular sieves. S-layer ultrafiltration membranes (SUM's) are fabricated in three steps. First, S-layer carrying cell wall fragments or self assembly products are dropped on micro-filtration membrane. S-layer protein is then cross linked with glutaraldehyde under $2x10^5$ Pa and Schiff bases are reduced with sodium borohydride. SUM's are used to filter protein solutions and studies have demonstrated that they are much more effective than synthetic ultrafiltration membranes.

Another application of S-layer proteins together with SUM's is the immobilization of biologic macromolecules such as emzymes or ligands [30]. S-layer proteins are also used for the immobilization of biologically active macromolecules. The carboxylic acid group of the protein construct is activated by 1-ethyl-3-(3-dimethylaminopropyl) (EDC) so that it could react with the free amino group of the enzymes, antibodies or ligands such as streptavidin or protein A.

Secondly S-layers are used in vaccine applications as both carrier and adjuvants since 1987. The research goes on mainly in three areas: immunotherapy of cancers, antibacterial vaccines, and antiallergic immunotherapy. In conventional vaccines the haptens or antigens are bound to a protein carrier but due to the state of the common carriers (monomers in solution or dispersed as aggregates on aluminum salts) a strong immobilization of ligands to the protein carrier cannot be done. S-layer proteins which have suitable functional groups for protein binding, are advantageous as immobilization matrices. [28,30]

S-layer proteins are also used in the stabilization of lipid membranes and liposomes. As currently 60% of drugs act on membrane proteins since they are key factors in the cell's metabolism. For that reason in the domains of drug discovery and biosensor fabrication, stabilizing lipid membranes with functional membrane proteins have become an important issue. Stabilization of lipid membranes with S-layer proteins is one of the most promising approaches. To mimic the biological structure of archaeal cell envelopes, S-layer proteins are generated on Langmuir lipid monolayers, planar lipid membranes or liposomes and than they are attached on one or both sides of lipid membrane. The processing of lipid monolayers inspirited by archaeal cell envelopes are schematically given in the figure 2.5.

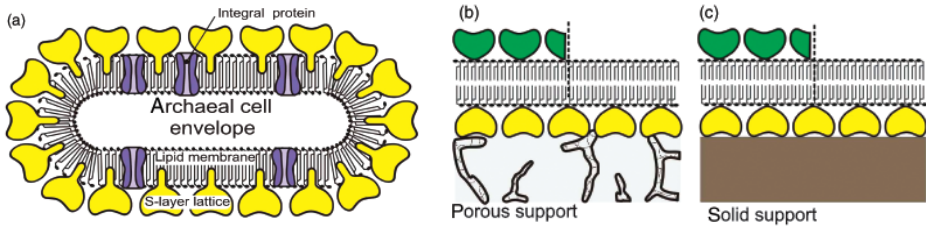

Figure 2.5: Schematic representation of various S-layer supported lipid membranes and their similarity with Archaeal cell envelope [29]

These membranes have proven to be stable at the long term hence they have the prospect to be used in many areas such as diagnostics, high-throughput screening for drug discovery, sensor technology, electronic or optical devices, and might even find application in DNA-sequencing.

The idea of using S-layer lattices in chemically depositing metal particles from a solution came from the investigation of mineral formation by bacteria in natural environments. To precipitate metal particles, S-layer structures self assembled on solid supports are exposed to metal-salt solutions. Lattice spacing and symmetry of the S-layer structure define the arrangement of nanoparticle superlattices. Moreover the morphology of the pores determine the morphology of nanoparticles since they are precipitated on the pore areas. Some early examples of generating nanoparticle superlattices are the precipitation of cadmium sulfide (CdS) by Shenton et al. [33] at 1997 with 4-5nm in size and gold particles formed under electron beam in a TEM by Dieluweit et al in 1998 [34]. This is an important progress because it allows the precise definition of areas where nanoparticles are deposited. Also, chemical

deposition of Pd and Pt from metal salts ($PdCl_2$ and $KPtCl_6$ respectively) on S-layer patterned surfaces have been accomplished by Mertig et al in 1999 [29].

Likewise biomineralization has become more and more important in the synthesis of inorganic materials exhibiting uniform particle size, morphology, oriented nucleation and assembly. S-layers may be used in this field as a precisely defined surface with exactly positioned nucleation sites for biomineralization Another approach of generating highly ordered nanoparticle structures is to use genetic engineering tools in order to construct a chimeric S-layer fusion protein with demonstrated biomineralization properties [35].

Crystalline arrays of nanoparticles can also be obtained with wet chemical methods on S-layer lattices, the control over the contact distances of neighboring particle surfaces and the particle size are essential for benefiting of the quantum phenomena. Hence the deposition of preformed nanoparticles onto S-layers may have a great advantage for the fabrication of nanometer sized electronic devices The use of S-layer proteins as an electrodeposition mask has been demonstrated by Allred et al [4]. Arrays of cuprous oxide (Cu_2O), Ni, Pt, Pd, and Co exhibiting long-range order with the 18nm hexagonal periodicity of the protein openings has been generated via electroless deposition. Based on these studies the *D. radiodurans* HPI layer has been proved to be a strong protein that remains structurally intact under a wide range of environmental conditions. Hence the electrodeposition of ordered nanostructures with a variety of superlattice symmetries can be achieved by S-layer proteins of various species.

2.3.6. Major S-Layer Possessing Bacterial Strains

S-layers are crystalline surface layers in prokaryotic organisms composed of protein or glycoprotein subunits. A S-Layer protein consist of identical proteins or glycoproteins of molecular mass 30-220 kDa. S-layers are connected to cell envelope structures such as peptidoglycan, pseudomurein or outer plasma membrabne.

The monomeric parts of S-layers constituting the subunits are coupled together and to the underlying cell envelope layers through non-covalent forces. When compared with other porous materials, S-layers having aligned functional groups with identical position and orientation constituent a perfect matrix [35].

Going from the inside of the cell as illustrated in figure 2.6, the envelope starts with a layer of intercalating material more or less 30nm thick. The majority of the proteins are water soluble. After the intercalating materials there is a "backing layer" responsible from maintaining the shape and structure of the envelope if there is no peptidoglycan layer. On the outer side of the backing layer there is the hexagonally packed intermediate (HPI) layer and finally a carbohydrate coat of considerable (approx. 40 nm) thickness is seen as the outermost layer. The schematic representation of the components of a prokaryotic cell envelope containing crystalline surface layers (S-layers) is seen in the figure 2.6. The major components of the molecular architecture of the Gram-positive cell envelope as observed in eubacteria and archaeobacteria (containing peptidoglycan or pseudomurein, respectively) are characterized in the figure.

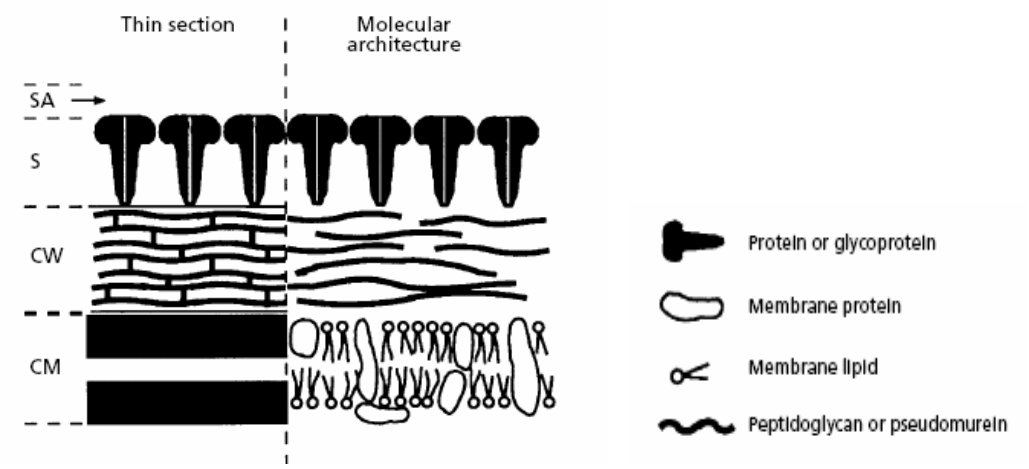

Figure 2.6: Schematic illustration of major classes of prokaryotic cell envelopes containing crystalline surface layers (S-layers) [38]

Some of the major nanobiotechnologicaly revelant S-layer containg organisms are *Deinococcus radiodurans* (previously *Micrococcus radiodurans*), *Bacillus sphaericus*, *Sporosarcina ureae*, *Bacillus stearothermophilus* and *Lactobacillus helveticus* (Table 2.4).

a) *Deinococcus radiodurance*

Previously called *Micrococcus radiodurance* is a bacterium famous in radiation biology for its extraordinary resistance to ionizing and ultraviolet irradiation. *D. radiodurans* was discovered in 1956 by Arthur W. Anderson at Oregon Agricultural Experiment Station in Corvallis [15]. The sequence of the *D. radiodurans* R1

genome has been determined in its entirety in 1999 (by O. White, The Institute for Genomic Research) [36]. *D. Radiodurans* strains and plasmids are given in the table 2.2 below.

While a dose of 10 Gy is sufficient to kill a human, and a dose of 60 Gy is sufficient to kill all cells in a culture of *E. coli*, *D. radiodurans* is capable of withstanding an instantaneous dose of up to 5,000 Gy with no loss of viability, and an instantaneous dose of up to 15,000 Gy with 37% viability. It can survive heat, cold, dehydration, vacuum, and acid, and because of its resistance to more than one extreme condition, *D. radiodurans* is known as a polyextremophile [37] .

Table 2.2: Bacterial strains and plasmids [36]

Deinococcus radiodurans	**Description**
R1	ATCC 13939
302	As R1 but uvA1 (mtcA)
res30	As R1 but *recA*
IRS1-IRS49	As 302 but ionizing radiation sensitive

Deinococcus radiodurans is a Gram-positive bacterium that forms reddish-pink colonies. Cells divide alternately in two planes and optimal growth occurs at 30°C. It is an ideal bacterium for patterning at very small scale (on the order of ~ 1 μm) because of its large pore size and lattice spacing. An average bacterium of 1.4 μm diameter possesses $2x10^4$ copies of HPI layer protein. Disassembling or reassembling S-layers to individual subunit proteins is not possible because purified S-layers proteins from *D. radiodurans* are chemically cross-linked.

Isolated cell walls layers except for the peptidoglycan and the HPI layer from *'Micrococcus radiodurans'* (Rl) can be dissolved by a treatment with SDS [36]. The procedure for isolating the HPI layer is based on this observation. If whole cells are exposed to detergent treatment the intercalating material, the backing layer and the carbohydrate coat are disintegrated and the HPI layer is released into the medium which can be separated from the 'stripped' bacteria by differential centrifugation [35,36].

The molecular mass of HPI layer protein is 655 kDa. The amount of HPI layer protein per cell is 0.0235 pg which is about 8 % of the total cell protein (0.29 pg) [34]. The HPI layer arranged on hexagonal lattice with a spacing of 18nm. Figure 2.2 illustrates an electron micrograph of a negatively stained HPI layer. The core which has a diameter of approximately 10nm is composed of two hexagons: an outer one (14nm) and an inner one (10nm). The larger hexagon is located on the smooth outer surface, the smaller one face the backing layer. The cores are interconnected in the lattice by "spokes" going out from the corners of the outer hexagon. A detailed summary of physical and chemical properties of HPI layer proteins is given in the table 2.3.

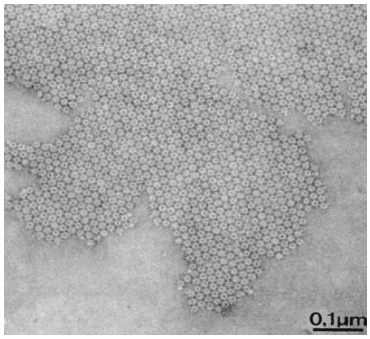

Figure 2.7: Electron micrograph of negatively stained HPI layer [35]

Table 2.3: Summary of physical and chemical properties of the HPI layer

Parameter	Value
Symmetry	p6
Lattice Constant	18nm
Layer Thickness	~6nm
Molecular mass per unit cell	~655
Molecular mass of (uncleaved) promoters	104kDa
Number of promoters per unit cell	6
Volume to molecular weight ratio	0.0026nm^3/Da

The applications of *Deinococcus radiodurans'* S-layers are fabrication of hexagonnaly patterned metal, metal oxide or other inorganic nano structures, patterning of biological macromolecules such as enzymes, protein receptors, or

nucleic acids and physical and thermal stabilization of lipid-based structures, such as membrane monolayers, bilayers, and vesicles.

b) Other bacterial strains

Bacillus sphaericus is a Gram-positive spore-forming aerobic bacterium which lives in soil and aquatic environments. It produces a toxin active against larvae of some mosquitoes. *B. sphaericus* generates a square patterned S-layer. The S-layers of *B. sphaericus* can be disassembled into monomers by chaotropic agents. *B. sphaericus* S-Layers are one of the best characterized of the S-Layer proteins. *B. sphaericus* S-layer's monomers will reassemble upon the addition of 10mM $CaCl_2$. The S-layers have square lattices with 12.5nm lattice spacing and 3.6nm pore size. The S-layer proteins are not cross linked and can be disassembled and reassembled.

The applications of *B. sphaericus* S-Layers are generation of square arrays of patterned metal, metal oxide, semiconductor, or other inorganic nanoclusters, patterning of biological macromolecules such as enzymes, protein receptors, or nucleic acids and physical and thermal stabilization of lipid-based structures, such as membrane monolayers, bilayers, and vesicles.

Sporosarcina ureae is a Gram-positive, motile, spore-forming coccus bacterium. This soil bacterium produces the enzyme urease, which breaks down urea to provide the organism with a source of nitrogen. Thus, it is thought to play a major role in urea decomposition in soil. *S. ureae* produces an S-layer having a square pattern, which can be disassembled into monomers using chaotropic agents such as guanidine HCl. These monomers will reassemble upon addition of 10mM CaCl2. The lattice spacing is 12.5 nm and the pore size is about 2.6 nm**.** They are not cross-linked so they can be disassembled and reassembled. The applications are mainly generation of square arrays of patterned metal, metal oxide, semiconductor, or other inorganic nanoclusters, patterning of biological macromolecules such as enzymes, protein receptors, or nucleic acids and physical and thermal stabilization of lipid-based structures, such as membrane monolayers, bilayers, and vesicles [38].

Bacillus stearothermophilus is a Gram-positive spore-forming bacterium, with an optimal growth temperature of 55°C. *B. stearothermophilus* produces multiple S-layers depending on physiological conditions. The protein cataloged here is the oblique S-layers produced when the organism is cultured under aerobic conditions.

This S-layer can be disassembled into monomers using chaotropic agents such as guanidine HCl. These monomers will reassemble by the addition of 10mM $CaCl_2$. The S-Layers show oblique parallelogram with lattice spacing: 11.6 x 8.6 nm and pore size about 5.1 x 1.7 nm. They are not cross-linked and can be disassembled and reassembled. They have the same applications with previous S-layers.

Lactobacillus helveticus is a Gram-positive, nonspore-forming lactic acid bacterium. It is used extensively in cheese making, serving as a culture ingredient for Swiss, Parmesan, Romano, Provolone and Mozzarella cheeses. S-layers of the organism form an oblique pattern that can be disassembled using lithium chloride, and can reassemble on various surfaces. S-Layer of *Lactobacillus helveticus* show oblique symmetry with lattice spacing 11 x 5.5nm and the pore size is about 3.5 x 2.5 nm. They are not cross-linked and can be disassembled and reassembled. They work well on glass and silicon. [38,39]

Table 2.4: Nanobiotechnologically relevant S-layer proteins [36,29]

Organism	S-Layer Protein	Molecular Weight (Da)	Lattice Type	Applications
Deinococcus Radiodurance	HPI	655000	Hexagonal	Generation of hexagonal arrays of patterned metal, metal oxide, semiconductor, or other inorganic nanoclusters
Geobacillus stearothermophilus	SbpB	94000	Oblique	Generation of oblique arrays of patterned metal, metal oxide, semiconductor, or other inorganic nanoclusters
Geobacillus stearothermophilus ATCC 12980	SbsC	121000	Oblique	
Bacillus sphaericus	SbsA	130000	Square	Generation of square arrays of patterned metal, metal oxide, semiconductor, or other inorganic nanoclusters

2.4. Biological Self-Assembly

2.4.1. Self-Assembly

The limitations of the conventional top-down approach such as size reduction problems, generating complex functional materials and over consumption of material and energy leaded to the newly known “bottom-up” approach. This idea involves designing functional materials via self-organizing molecules without any external intervention.

Fabrication at molecular scale had a significant impact on many technology fields such as electronics, biotechnology and medical science over the last ten years.

The scaling down in the modern electronics is going from microelectronics towards molecular electronics which increase their efficiency. Hence the key factor of the bottom-up approach being “self-assembly”, it is crucial to understand its principles [39].

Self-assembly can be described as an independent association of the components of a system into patterns or structures without any intervention from the outside world. The self-assembly scale is ranged from molecular crystals to planetary systems such as weather systems. To say that self-assembly is the connection between reductionism with complexity and emergence would not be overstated.

Self-assembly have many reasons to attract interest. First, since living cells self-assemble in many forms thus it is obvious that understanding life necessitates understanding self-assembly. Second, self-assembly seems to be the most appropriate strategy to construct nanostructures and consequently it will be a crucial part of nanotechnology. Third, applications of self-assembly may be useful in robotics, smart materials and manufacturing self healing structures or computer networks. Finally, separate components of a system can be linked to many interacting component of the same system via spontaneous development of patterns.

Since the term “self-assembly” is excessively used at a point that it is almost synonymous with “formation” a clear definition to draw the limits of the self-assembly process has to be done. Therefore, reversible processes involving pre-existing components of a disordered structure and allows a precise control over those components are called self-assembly [40].

Basically self-assembly processes can be divided into two classes being static and dynamic self-assembly. Systems are at the equilibrium state in the former, there is no change in the energy. For instance molecular crystals and globular proteins are static self assembly systems. To achieve the static self-assembly stage the system requires energy but after while it becomes entirely stable. The majority of research has centralized around this type. The second one can be described as dynamic self-assembly. This is a more complex phenomena and it involves energy for the formation and maintaining of the structures or patterns. Some examples are chemical

reactions oscillating between reaction and diffusion or biological cells. The research on this type of self-assembly is only at its beginnings.

In addition two sub class of the self assembly can be determined. One of them is "template directed self-assembly". In this type the structures and the forms are determined via interactions between the components and regular features in their environment. For example, the morphology of recrystallized structures onto surfaces is determined by the surface properties. The second type is "biological self-assembly". This phenomenon generate structures much more complex in terms of their function and morphology.

The definition of molecular self-assembly is the spontaneous organization of molecules at nearly thermodynamic equilibrium state [41]. As a result well defined and stable arrangements of molecules onto a substrate surface can be obtained. Molecular self-assembly make use of non covalent or weakly covalent forces (e.g. Van der Waals, electrostatic, and hydrophobic interactions, hydrogen and coordination bonds). On the other hand, self assembly at meso- or macroscopic scale involves interactions which are not valid in the case of molecules, such as gravitational attraction, magnetic fields, capillary and entropic interactions.

Molecular self-assembly is abundantly seen in nature. For example the silk assembly is a good known one. The monomeric silk fibroin protein is approximately 1 mm but a single silkworm can spin fibroins into silk materials over 2 km in length, two billion times longer. Similarly, spiders are another example of natural engineers who can construct many types of spider silks through self-assembly with remarkable strength and flexibility. These building blocks are often at the nanometer scale.

Much more sophisticated structures can also be build up via molecular self-assembly such as collagen and keratin which can self-assemble into ligaments and hair respectively. Also chaperone proteins assemble into a distinct ring structure to reform, fold and refold proteins. Seashell bio-mineralization is another example of well-known protein assembly system as well as mammalian tooth generated through self-assembly of a protein scaffold capable of recruiting calcium ions to specific sites for bio-mineralization [42]

Since the components of a self-assembly system should be mobile, it generally occurs in liquid phase or on smooth surfaces. The use of templates or controlled

environments can modify and/or control the self-assembly process. Usually the equilibrium state for the components should be attaint in order to adjust their positions relative to each other in the system.

Since molecular fabrication involves also the knowledge of surface science, to understand only molecular self-assembly is not sufficient to completely cover up this area. Materials interact with each other and with their environment via their interfaces hence the interfacial properties influence molecular mechanisms of micro- or nano-fabrication, interactions in molecular self-assembly, in `guest-host' molecular recognition and in molecular biomimetics [40-43].

2.4.2. Self-Assembly via Peptides and Their Application in Bio-Nanotechnology

Mimicking Mother Nature's ways of creating life seems to be the way to the future of material fabrication either in macro- or nano-scale. Biological constituents of life, such as phospholipid molecules, amino acids and nucleotides have not been thought as useful materials for materials science and engineering. However, among natural materials with the potential to be used in creating new generation materials peptides have a special promise because of their structural simplicity, diversity in chemical morphological means, physical and chemical stability and the possibility to be synthesized in large amounts [43].

To create molecular and macrobiological materials the basic requirements are chemical complementary and structural compatibility. As well as self assembly, they both need weak and non-covalent interactions to be attaint. Since self-assembly is a dynamic and reversible process hence it is not possible to design novel biological material without a complete understanding of the self-assembly process.

Two of the important kinds of self-assembled peptide used in bio-nanotechnology are Lego TM peptides and various Modulus peptides discovered both by Zang et al [43] Lego TM peptides are named after their structural properties resembling lego bricks involving well defined pegs and holes at nanometer scale. Zuotin, the first lego peptide is coming from a segment in a left-handed Z-DNA assemble into nanofibers [44].

Modulus peptides possess two different sides, one hydrophilic the other hydrophobic. Thus they can self-assemble in water. The leading force in peptide self-assembly is

the intermolecular interactions whereas in protein folding intramolecular ones drive the process. The lego peptides form ionic bonds on hydrophilic surfaces. [41-43]

Proteins having specific binding properties to inorganics can be generated via a new approach called “molecular biomimetics” [3] Usually, inorganic binding peptides are selected either by extraction from hard tissue, theoretically designing or by recombinant approaches. However the most practical and successful one revealed to be using combinational biology based molecular libraries.

Molecular recognition, self-assembly and genetic manipulation are the main tools of creating protein based material systems. Firstly nucleation, growth and morphology definition of inorganics are mainly determined by molecular recognition. Following molecular recognition the peptides self-assemble on the surface which leads to the formation of a supramolecular architecture. Finally since proteins are genetically coded it is possible to manufacture modified/engineered peptides in order to give them specific functions. A great number of application potential exist for this class of biological materials such as scaffolding for tissue repair and tissue engineering, drug delivery of molecular medicine, as well as biological surface engineering.

The main advantage of genetically engineered proteins for inorganics (GEPI’s) is their skill to guide and assemble functional molecules and nanoparticles. Geometrical shape of molecules can be controlled through inorganic-binding proteins in a way like the morphogenesis in hard tissues. Some other applications of such proteins can be cited as biosensors, diagnostic tools in medicine and cancer therapeutics. Implant designing, hard-tissue engineering, genomics and proteomics are areas which also benefit from protein adsorption and from interactions at solid substrates. Furthermore, hybrid materials for nanoscale electronics, magnetics and photonics can be produced via engineered peptide chains with specific affinity to nanaoparticles and functional molecules [3]. Figure 2.8 capitalizes the major application areas of GEPI’s.

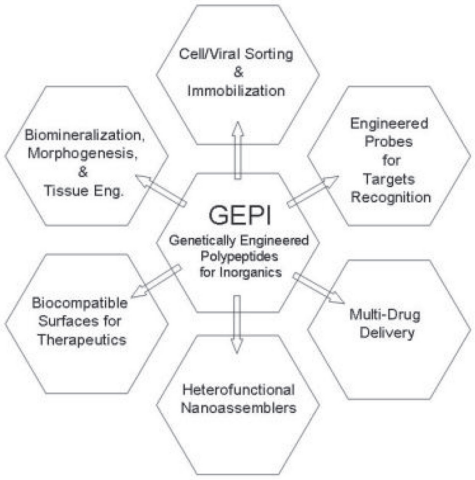

Figure 2.8: Potential Application areas of GEPI in the new field of molecular biomimetics [3].

To sum up, utilization of proteins and peptides as molecular erectors can be a way to develop novel materials and systems at molecular or nano-scale levels through their controlled binding to inorganics and their self-assembly properties on the technologically important surfaces. The control and understanding of the sequence–structure–properties relationships of these molecular systems is very important for the potential of peptide self-assembly. With the ability to fabricate three-dimensional assemblies with spatial precision, one can modify also the function. A great interest in the fabrication of nanoscale devices and demand for miniaturization necessitate progress in this area.

2.5. Electropolishing

2.5.1. Basic Principles

Electropolishing, is an well-known treatment for the smoothening of metallic surfaces. The basic principle of electropolishing is etching the surface in an acid bath and appliying an electric field simultaneously to the surface which causes a current flow. Due to this electric field sharp tips on the surface are removed preferentially. Electropolishing tends to flatten out roughnesses on a short wavelength scale, whereas long wavelength features remain. For most metals a similar voltage-current curve (see Figure 2.9) for the electropolishing process can be established.

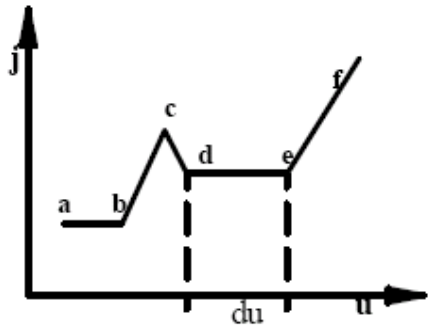

Figure 2.9: Current versus volage curve showing different stages of metal surface modification [44]

In the range (a-c) a relatively strong oxide layer is forms on the surface. At higher voltages (c-d) this layer is removed while the polishing process begins. In the range (d-e) the current is nearly independent of the applied voltage. The temperature of the electrolyte influences strongly the width of this plateau. At higher voltages (e-f) gaseous oxygen is set free at the anode, i.e. the surface to be polished causing serious discontinuities on the surface. For optimum polishing results the process is kept in the plateau region (d-e) and voltages above should delicately be avoided. Moreover, the detailed shape of the curve is dependant of the surface area ratio of cathode and anode and also on the initial surface roughness [47].

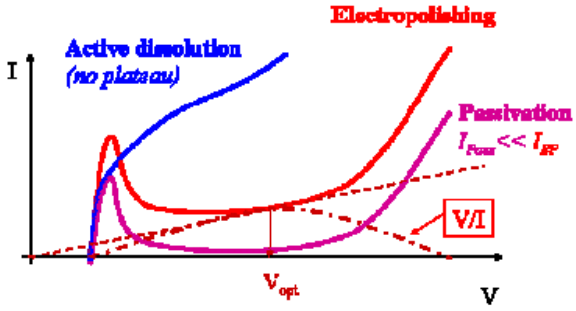

Figure 2.10: Current voltage curves for different situations [45]

A schematic current voltage curves are seen in figure 3.2 for various typical situations:

- Active dissolution which happens when no viscous layer is formed and the metallic ions dissolve freely in electrolyte;

- Passivation, where a stable, insoluble film forms on the surface and it prevents further corrosion;
- Electropolishing, where the current is limited with an interface layer (viscous layer) [48].

Often electrobrightening and electropolishing are considered as different processes: In the first case the objective is to have a moderate smoothing action. The action is neither intense nor speedy. It happens at low current densities of 300-500 A/m^2, 2-12 μm are removed and the typical duration time is between 20 to30 min.

On the other hand electropolishing deals with abrasion and scratches on the surface. The electrochemical action is, therefore, more intense and necessitates higher current densities of the order of 1000-3500 A/m^2. More metal is removed, 30-40 μm in a few minutes [45].

2.5.2. Electropolishing of Aluminum

Aluminum metal shows many oxidation reactions by a lot of aluminum surface treatments. The chemistry of the solution determines the treatment characteristics. In electropolishing process the polarization of the aluminum and the attack of the solution are optimized in such a way that a limiting oxide film is formed on the aluminum substrate. The dissolution rate and film thickness may widely vary during electropolishing.

The film formed on the aluminum substrate is important because it avoids crystallographic etching by the substitution of dissolution of metal atoms according to their energy, i.e. the position they have in the crystal lattice, by the dissolution according to their access and the characteristics of the oxide layer. Under the conditions of electropolishing the reaction products are carried away from the surface via a slow diffusion and this controls the dissolution process of the metal. Due to the continuous film growth and dissolution the points of access of the electrolyte are constantly changing thus the dissolution takes place at different points and the metal atoms are, therefore, attacked more or less at random which results a smoother surface. The porosity, electrical properties and the thickness of the film prevents etching. The film which is formed under electropolishing conditions is qualitatively similar to the one that is produced in the anodizing process [46].

For the electropolishing of aluminum different processes have been established. Some of them are listed in table 2.4 below.

Table 2.5: Major electropolishing process of aluminum [47]

Process Name	Brytal	Alzac	Phosphoric Acid
Contents	Sodium carbonate 12-20 % Trisodium phosphate 2.5-7.5 %	Fluobotic acid 2.5 %	Sulphuric acid 4-45 % Phosphoric acid 40-80 %
Temperature	75-95° C	30° C	70-95 ºC
Voltage	7-16V	15-30V	7-15V
Current Density	2-5 A/dm2	1-2 A/dm2	2.7-100 A/dm2
Time	10-30min	5-10 min	20 min
Application	Pure aluminium Decorative work	Reflectors	Replace mechanical polishing

3. MATERIALS AND METHODS

3.1. Materials

3.1.1. Bacterial Strain Deinococcus radiodurans

Deinococcus radiodurans SARK (ATCC35073) was purchased from American Type Culture Collection.

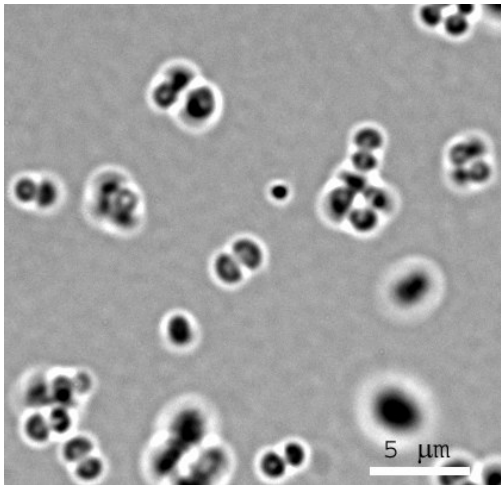

Figure 3.1: Brithfield migrograph of Deinococcus *radidurans* cells [39]

3.1.2. Bacterial Culture Media

The medium (TGYM) for the bacterial growth of *Deinococcus radiodurans* was prepared as defined by the American Type Culture Collection (ATCC). 10gr tryptone (LABM), 3gr yeast extract (LABM), 1gr glucose (MERCK) and 0.5gr l-methionine (MERCK) were dissolved in distilled water and completed to 1 liter in a graduated flask. The sterilization of the bacterial culture media was accomplished at 121°Cfor 15minutes using Zirbus Technology steriline.autoclave.

3.1.3. Inorganic Substrate Materials

3.1.3.1. (100) Oriented Silicon Wafer

Polished Si (100) wafers with a native oxide layer were used as substrates for the recrystallization experiments. Any chemical or either mechanical treatment was applied to he silicon wafer samples. However, to realize atomic force microscopy

studies on recrystallized S-layer lattices, the silicon wafer discs were cut into small pieces approximately in the order of 1cm by 1cm before all processing steps.

3.1.3.2. Mica

Single crystal (001) muscovite mica sheets obtained from Ted Pella Inc. were used in the recrystalization experiments.

3.1.3.3. Aluminum

Aluminum specimens were supplied from ASSAN Aluminum A.Ş. Aluminum surfaces were heat treated before any further steps. Foratomicforce microscopy studies aluminum specimens were cut onto little pieces (approximately 1cm by 2cm).

3.1.4. Stock Solutions and Buffers

3.1.4.1. Glycerol Stock Solution

50% (w/v) glycerol (MERCK) was mixed with distilled water and completed to 100 ml in a 250 ml Erlenmeyer flask.

3.1.4.2. Detergent Stock Solution

5% (w/v) sodium dodecyl sulfate (SDS) (MERCK-Schuchardt) was used as detergent stock solution.

3.1.4.3. S-layer Protein Stock Solution

S-layer stock solution was prepared from detergent solution with a mixture of purified S-layer proteins. The concentration of the solution was adjusted to 0.1-1 mg/ml. The protein stock solution was kept at room temperature in 5% SDS until further use.

3.1.4.4. SDS-PAGE Buffers

The compositions of separating gel solution and the stacking gel solution are given in the table 3.1a and 3.1b below.

After gel electrophoresis staining and destaining buffers were used in the SDS-PAGE process.Staining buffer consist of %0.1 Coomassie brilliant blue, %50 Methanol and 12% glacial acetic acid. Destaining buffer is composed of 30% methanol and 7% acetic acid. Unstained protein molecular weight marker (#SM0431) (Fermantas) was used.

Table 3.1: Separation gel composition for SDS-PAGE and Stacking gel composition.

A. Separating Gel (5ml)	
dH2O	1,6
30% - %8 (w/v) Acrilamid:bisacrylamide	2
1.5M TRIS	1,3
10% SDS (w/v)	0,05
10% APS (w/v) (ammoniumpersulfate)	0,05
TEMED	4µl

B. Stacking Gel (2ml)	
dH2O	1,4ml
30% - %8 (w/v) Acrilamid:bisacrylamide	0,33ml
1,0M TRIS	1,3ml
10% SDS(w/v)	0,02ml
10% APS(w/v)	0,02ml
TEMED	2µl

3.1.5. Aluminum Surface Treatment Solutions

3.1.5.1. Mild Etching Solution

10% NaOH in deionized water was used as the chemical mild etching solution.

3.1.5.2. Electropolishing Solution

The electropolishing solution was prepared from sulfuric acid (10%), phosphoric acid (%60), nitric acid (%1) and deionized water (%29).

3.1.6. Lab Equipments

Autoclaves **:** Zirbus Technology Steriline, LTA300
2540 ML benchtop autoclave, Systec GmbH Labor-Systemtechnik.
: NuveOT 4060 vertical steam sterilizer, Nuve.

Balances **:** Precisa BJ 610C, order# 160-9423050,
: Precisa XB 220 A, order# 320-9204-001,
Precisa Instruments AG Dietikon.

Centrifuges **:** Avanti J-30I, Beckman Coulter.
: Sigma LAB centrifuge
: Microfuge 18, Beckman Coulter.

Centrifuge rotors **:** JA30.50Ti, Beckman Coulter.

Centrifuge Tubes	**:** Beckman 50ml
Deep freezes and refrigerators	**:** Heto Polar Bear 4410 ultra freezer, JOUAN Nordic A/S, catalog# 003431.
	: 2021 D deep freezer, Arcelik.
	: 1061 M refrigerator, Arcelik.
Incubators	**:** EN400, Nuve.
Magnetic stirrer	**:** AGE 10.0164, VELP Scientifica srl.
	: ARE 10.0162, VELP Scientifica srl.
Pipettes	**:** Pipetteman P10, P 100, P1000, Eppendorf.
pH meter	**:** Inolab pH level 1, order# 1A10-1113, Wissenschaftlich-Technische Werkstätten GmbH & Co KG
Optical Profilometer	**:** Wyko DMEMS NT1100
Microplate Reader	**:** Bio-rad model 3550
Atomic Force Microscopy	**:** Ntegra Prima

3.2. Methods

3.2.1. Growth of Bacterial Culture

The bacterial culture of *Deinococcus radiodurans* was routinely grown at 35°C in the culture medium in 500ml shake flasks with continuous shaking at 220 rpm. Exponentially growing bacteria were collected after 10 to 12 h of growth at an optical density of 0.5 to 0.7 at 600 nm at the early stationary phase of growth.

3.2.2. Characterization of D. radiodurans

3.2.2.1. Growth Curve

a) Generation of the growth curve

Samples were taken hourly from the growing bacterial culture and optical density was measured at 600nm using an optical spectrophotometer.

b) Calculation of doubling time and growth rate

Since the $\log_{10}$ curve appears linear over the time period 240-720 minutes, the doubling time was calculated by replotting the data over this period and converting the A_{600} values into $\log_2$ values.

3.2.2.2. Quantification of Total Proteins

The amount of the total protein was determined according to the Bradford method. First, a dilution series of calibration standards were prepared in the solvent to cover the range 150 to 750 µg protein/ml. Bovine serum albumin (BSA, 2.0 mg/ml) was used as calibration standard and a calibration plot was established using these values.

The protein samples of 5µl were dropped in the microplate and 250µl of Bradford reagent was added on top of every sample including standard solutions. The microplate was shaken for 30sec in a microplate shaker and then incubated for 15min at room temperature. The color change produced when the dye binds to proteins provides a measure of the total protein amount. The absorbance of the sample, calibration standards, and reference standard was measured at 595 nm (A_{595}). The procedure is schematically illustarated in Figure 3.1

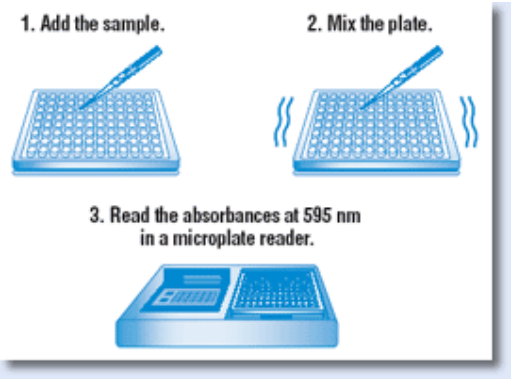

Figure 3. 2: Schematic description of the total protein assay's steps from Pierce

Coomassie dye (Brilliant blue G250) binds to protein molecules in acidic pH by two means. The triphenylmethane group binds to nonpolar structures in proteins, and the anion sulfonate groups interact with protein cationic side chains (e.g., arginine and lysine side chains) in acidic pH. The protein concentration of the sample was determined by interpolation from the calibration plot.

3.2.2.3. Determination of Cell Dry Weight

Cell dry weight measurements were performed as follows: First, the eppendorf tubes were placed in the incubator and left overnight. They were placed in the desiccator for 2 hours and then weighted out. The bacterial culture was centrifuged at 8000 rpm (Beckman centrifuge, Allegra® X-22) for 5minutes to collect the cells. The

supernatant was removed and the eppendorf tubes containing collected cells were placed in the incubator at 80 °C and left overnight. Then the total weight of cells and the eppendorfs were measured and the cell dry weight was calculated by substracting the bare tube weights from the measured total weights.

3.2.3. Purification of S-layer Proteins

The basic purification principle of s-layer proteins is to break the hydrophobic interactions by which HPI layer is connected to the bacterium upon detergent addition.

1L culture of *Deinococcus radiodurans* SARK (ATCC 35073) was grown to early stationary phase in TGYM medium. Cells were harvested in the early stationary phase of growth. They were sedimented at 2200 g for 5 min then washed twice with ddH2O and resuspended in 5% SDS. The suspension was incubated at 60 °C in a rotary shaker with 220 rpm for 2 h to release HPI layer proteins. Under these conditions it is expected that the membraneous 'backing layer' and the intercalating material are dissolved and the HPI layer sheets are released into the medium. Denuded cells were twice sedimented by centrifugation at 2200 g for 15 min and discarded. HPI layer proteins were obtained by centrifuging the supernatant at 18 000 g for 45 min and the protein pellet was resuspended in 5% SDS.

The concentration of S-layer proteins was determined using Bradford method as described previously and adjusted to 0.1-1µg protein/ml for optimal surface coverage.

3.2.4. Characterization of S-layer Proteins

SDS-PAGE method was performed for characterization of S-layer proteins. Sodium dodecyl sulfate (SDS) is an anionic detergent. When it is dissolved its molecules have a net negative charge within a wide pH range. A polypeptide chain binds amounts of SDS in proportion to its relative molecular mass. Protein separation by SDS-PAGE can be used to estimate relative molecular mass, to determine the relative abundance of major proteins in a sample, and to determine the distribution of proteins among fractions.

The SDS-PAGE analysis of purified S-layer proteins was accomplished based on the literature data (Maniatis Molecular Cloning). Gels were prepared at as previously indicated amounts. Bio-Rad mini protean SDS-PAGE kit was used to pour out the

gels. Electrophoresis current was 80V until the end of the stacking step, afterwards during the separating step the current was 160V. The electrophoresis time was about 90 minutes. The gels were than immersed in the staining buffer and placed on a shaker. Destaining buffer was applied to the SDS-PAGE gel after 2 hours.

3.2.5. Surface Treatment of Aluminum

3.2.5.1. Pretreatment of Aluminum Surface Before Electropolishing

The aluminum sheets were annealed at 350°C for one hour at ambient atmosphere. The annealing is necessary for obtaining large and uniform grain sizes and reducing internal stresses before electropolishing of the aluminum.

3.2.5.2.Surface Preparation Prior to Electropolishing

The aluminum surface is usually received rather clean and free from surface contamination. Nevertheless, the surface of rolled aluminum sheets may still be contaminated to a certain degree by oxides. Thus, a specific cleaning process is required to be carried out to provide a uniform chemically active surface. The surface must be chemically cleaned by controlled etching to remove oxides in order to obtain a surface which will provide a uniform base for electropolishing. In addition to contaminants, aluminium oxides of various forms may be present on the surface. These oxides have to be removed and replaced by a uniform oxide surface, otherwise they can produce unexpected results during the later surface treatments. It involves the dissolution of the aluminum surface layers, oxides via a small amount of etching and leaving the thin oxide coating previously present in a uniform condition [49].

The solvent cleaning was realized by immersing the samples in ethanol for 1 to 2 minutes and washed with deionized water to remove effectively grease and oil contaminations.The chemical cleaning of aluminum was performed in 10% NaOH solution.

When the aluminum is immersed in caustic soda the surface is progressively dissolved and it is microscopically roughened. On this surface a large number of small pits or depressions are developed which causes a matt or dull appearance due to the scattering of reflected light.The chemical etching process is based on the amphoteric character of aluminum. While aluminum is oxidized to form aluminate anions, hydrogen evolution occurs.

$$2\ Al + 2\ NaOH + H_2O \Rightarrow 2\ NaAlO_2 + 3H_2 \quad (3.1)$$

$$2Al + 2OH^- + 6H_2O \Rightarrow 2\ Al(OH)^{4-} + 3H_2 \quad (3.2)$$

The deposition reaction:

$$2\ NaAlO_2 + 4\ H_2O \Rightarrow 2\ Al(OH)_3 \downarrow + 2\ NaOH \quad (3.3)$$

After the chemical cleaning step, aluminum was washed with deionized water and subsequently immersed in 5 % HNO_3 solution for a few minutes and then washed twice with deionized water [50].

3.2.5.3. Electropolishing Procedure of Aluminum

Electropolishing is defined as controlled electrochemical dissolution of the high spots and the depressions of metal. As a result of this selective dissolution, a mirror-bright surface can be created. The surface atoms of the metal areremoved by applying an external power supply.

Aluminum samples were placed as anode in the process. The cathode was a graphite rod placed approximately at 3mm of the anode. The schematic representation of the electropolishing setup is presented in Figure 3.2. The electropolishing process was performed in a glass beaker containing the electrolyte at temperatures between 80-90°C. The optimum current density was 0.2A/cm^2. The electrolyte was mixedvigorously with a magnetic stirrer. The mixingsprevents the formation of oxygen bubbles on the surface which effect the homogeneity of the polishing process.

Table 3.2 : Electropolishing conditions optimized via experimental methods

Electropolishing Recipe for High Purity Aluminum				
Electrolyte Concentration	**Current Density**	**Temperature**	**Time**	**Agitation**
%60 H_3PO_4	~0.2A/cm^2	80-90C	5-10min	Yes
%10 H_2SO_4				
%1 HNO_3				
%29 dH_2O				

Electropolishing time was approximately 5 to 7 minutes. The samples were immersed in dH_2O immediately after they have been removed from the electrolyte in order to avoid the acid further eating the metal.

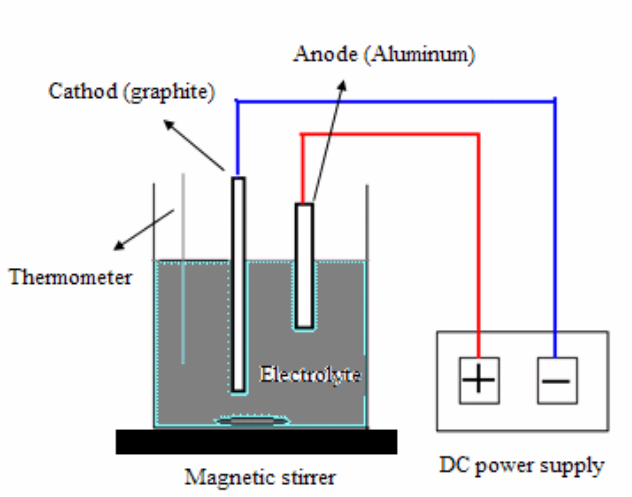

Figure 3.3: Schematic representation of the electropolishing setup

3.2.6. Characterization of Polished Aluminum Surfaces

The roughness of polished aluminum surfaces were investigated using both optical profilometer and atomic force microscopy.

For optical profilometer experiments Wyko DMEMS NT1100 Optical Profilometer at Metallurgical and Materials Engineering Laboratories in Istanbul Technical University was used. Different areas ranging from $3um^2$ to $10um^2$ were analyzed and surface roughness was measured as Ra (Roughness average) or Rq (the equivalent of RMS -- Root Mean Square) values.

Atomic force microscopy investigations were performed with Ntegra Prima AFM at Genetic Engineering Department Laboratories in Istanbul Technical University. Silicon nitride probes with typical curvature radius of 10nm were used. The scan rate was 1.5 Hz.

3.2.7. Nanotemplate Formation on Inorganic Substrates by Using S-layer Proteins

S-layer protein stock solutions were stored at room temperature in eppendorf tubes until use. Prior to coverage procedure, tubes were shaken several times for preventing proteins to precipitate at the bottom of the tubes.

Si wafer substrates were first cleaned in acetone, than in ethanol, both ultrasonically. The samples were than immersed in ultrapure water. Finally, they were allowed to air dry and than brought into contact with the protein solution.

Mica substrates were cleaved before each procedure by a Scotch tape and than were contacted immediately to the protein solution.

Aluminum samples were electrochemically polished first and than cleaned in ethanol in an ultrasonic bath prior to any contact with the protein solution.

Nanotemplates were formed on the inorganic substrates by using two different techniques depending on the type of the substrate material. The nanotemplate formation techniques are schematically illustrated in Figure3.3.

In the first technique, a small sample of inorganic material was immersed into the eppendorf tube containing S-layer solution. This technique was mostly applied for silicon wafer pieces and cleaved mica. The eppendorf tubes were kept laterally through the whole coverage procedure during time periods from 2 up to 60 minutes according to the literature data [4] .

The second technique was applied to aluminum samples because of the size limitations of the aluminum pieces. 50µl of the protein stock solution was pipetted out onto the substrate surface and dried out at room temperature.

Following protein coverage, all samples were washed twice with ultrapure water and dried with nitrogen gas blow before atomic force microscopy investigations.

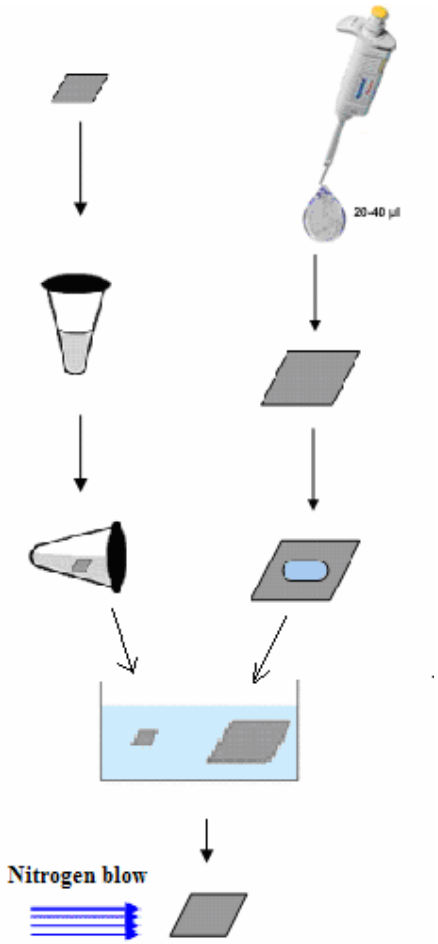

Figure 3.4: Schematic representation of nanotemplate formation by s-layer proteins

3.2.8. Characterization of Nanotemplated Surfaces via Atomic Force Microscopy

AFM images were taken at Molecular Biology and Genetics Laboratories at Istanbul Technical University with Ntegra Prima AFM equipment.. Semi-contact mode was performed to visualize surface topography. The scan rate was varied between 0.5-1.6 Hz under ambient conditions. Scanning probe tips used were all silicon nitride with 1,6x3,6x0,4mm standard sizes. The tip height was 10 to20um.

4. RESULTS AND DISCUSSION

4.1. Growth Characterization of Deinococcus radiodurance

4.1.1. Growth Curve and Cell Dry Weight Results

In order to investigate the growth characteristics of *Deinococcus radiodurans* cells were grown in 500ml shake flasks. 1,5 milliliter samples were taken from three different shake flasks (control samples) every hour and their absorbance values were analyzed using optical spectrophotometer to follow growth characteristics of the bacteria. The growth curve of *Deinococcus radiodurans* (figure4.1) was plotted according to the values obtained by optical spectrophotometer.

The four characteristic phases of the growth curve was observed in the growth curve of. *Deinococcus radiodurans.*

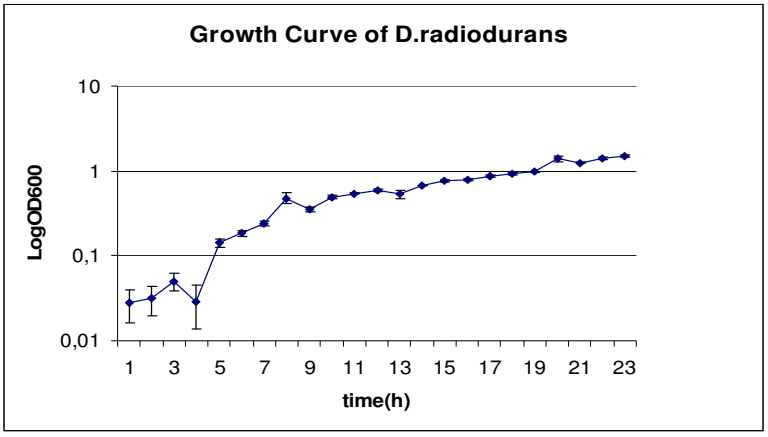

Figure 4.1: Growth Curve of *Deinococcus radiodurans*

As seen in the figure 4.1 the lag phase starts immediately after innoculation into the fresh medium. The bacterial cell population remains temporarily stable for the five hours. The exponential phase of growth starts at the 5th hour of the incubation. This phase shows balanced growth wherein all the cells are dividing regularly and are growing by geometric progression. The division of cells occurs at a constant rate and depends on the composition of the growth medium and the conditions of incubation. The third phase is the stationary phase. Since the exponential growth is limited in a

batch culture (e.g. a closed system such as a test tube or flask) after the 10th hour of incubation the bacterial population enter into the stationary phase.

According to the literature data [allred], bacterial surface layers are structurally intact and more abundant at the early stationary phase. Hence it was important to determine the growth characteristics in order to obtain the optimum protein quality for further applications.

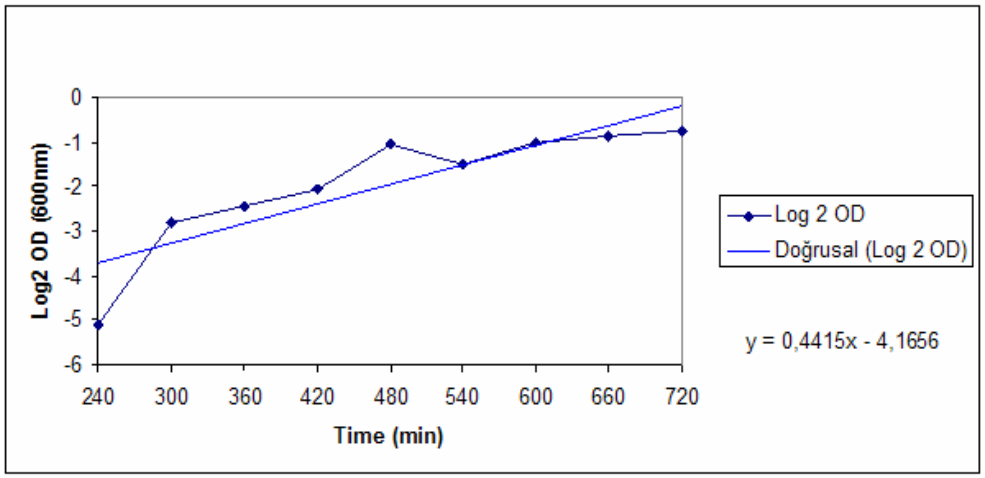

Figure 4.2: Determination of doubling time and growth rate

The rate of exponential growth of a bacterial culture is expressed as generation time (also called the doubling time) of the bacterial population. Generation time (G) is defined as the time (t) per generation (n = number of generations). Hence, G=t/n is the equation from which calculations of generation time (below) derive.

To calculate the growth rate the linear part of the growth curve was replotted and the values of optical density were converted into $\log_2$ values. The slope of the line calculated via its equation gives directly the growth rate which is given in the figure 4.2 above is equal to 0,4415 $(A_{600})_2$ per minute. The doubling time is the inverse of this value (1/ 0,4415) which is equal to 2,26 minutes.

The mass of cells during the growth were also identified by using dry cell weight method. The results are presented in Figure 4.4 and indicates that the yield was 0.6mg at early stationary phase of the bacterial growth .

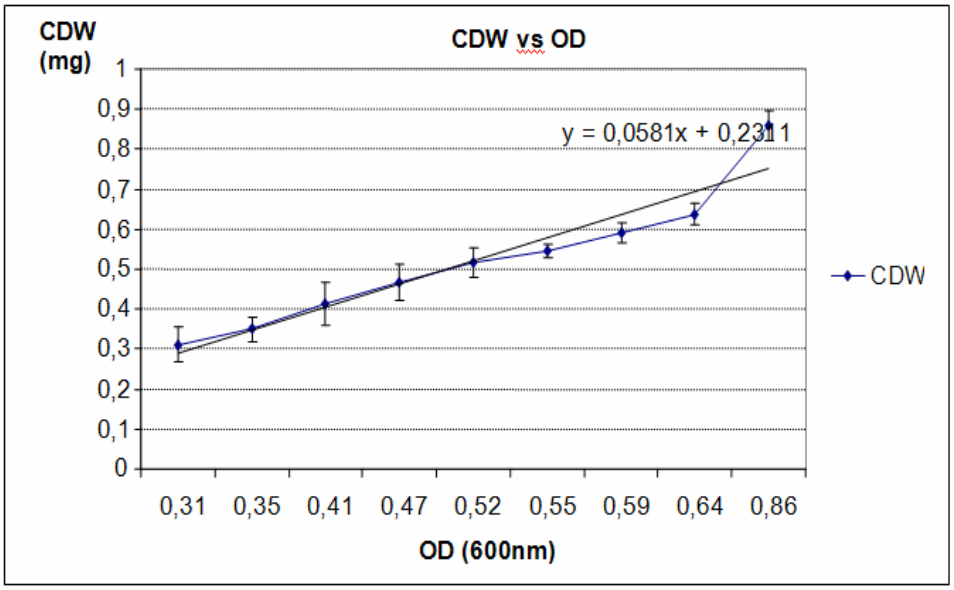

Figure 4.3: Cell dry weight analysis versus optical density

4.1.2. Analysis of Total Proteins

We performed a total protein analysis to understand level of protein production in different phases of growth. Three samples from the bacterial culture media were taken at 9th,11th and 13th hours of incubation and they were analyzed to determine the total amount of protein as described in the methods section.

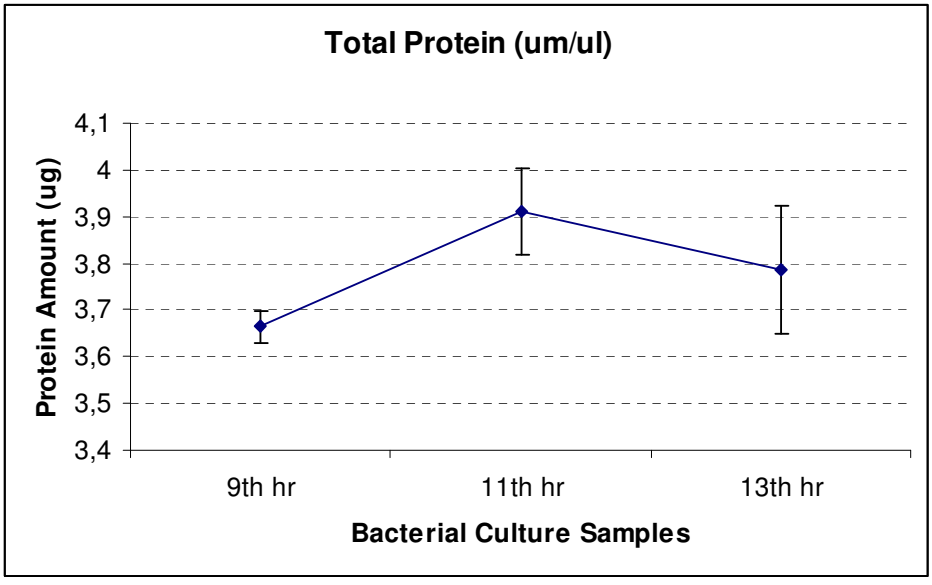

Figure 4.4: Total protein assay

Table 4.1: Total protein amounts of bacterial samples

Bacterial Culture Samples	Protein amounts (µg/µl)
+09h (1)	3,69
+09h(2)	3,63
+09h (3)	3,67
+11h (1)	3,96
+11h (2)	3,97
+11h (3)	3,80
+13h (1)	3,94
+13h (2)	2,69
+13h (3)	3,72

The maximum protein production was reached around the 11^{th} hour of bacterial growth, which corresponds to the beginning of the stationary phase. Therefore cells were collected after 11 hour incubation time to extract the optimum S-layer protein quality.

4.2. Characterization of S-Layer Proteins

Bacterial culture of D. radiodurans was routinely grown at 30ºC with continuous shaking at 220rpm. S-Layer proteins were harvested at the early stationary growth phase and then purified as described in the methods section.

The presence of the major HPI layer proteins was demonstrated using SDS_PAGE method. The process was performed with a discontinuous buffer system in the presence of $NaDodS0_4$.

The presence of nine major bands corresponding to molecular weights ranged from 14 kDa to 104 kDa was observed upon commassie blue staining (Figure 4.5). Detergent extraction of the whole cell in 5% $NaDodSO_4$ yields upon PAGE a band pattern which shows at least the major HPI layer bands :104kDa and 91kDa

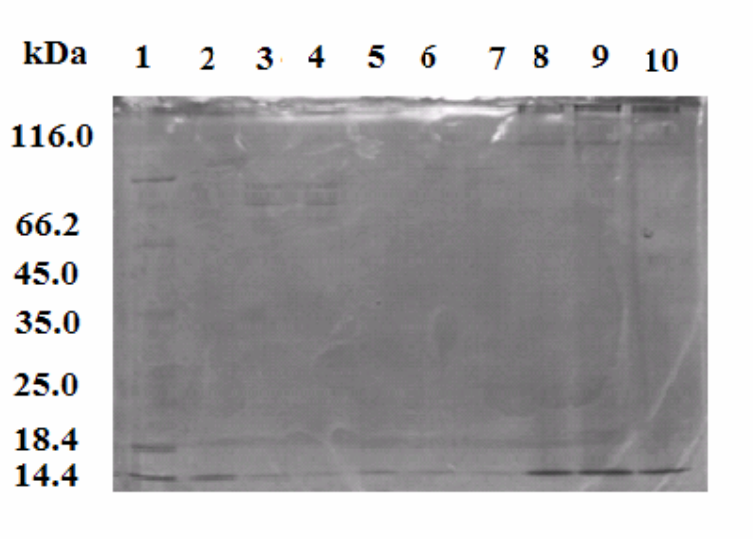

Figure 4.5: Analysis of a standard HPI layer preparation detergent extraction of whole cells at 60°C by SDS-PAGE

The first column shows the markers. The columns 2, 3 and 4 are detergent extracted S-layer proteins. The columns 5, 6, and 7 shows the remaining proteins in the supernatant solution after extraction procedure. Finally the columns 8, 9 and 10 are the cell pellets denuded from HPI layer proteins.

The total protein content of the standard HPI layer solution after purification was also determined using Bradford method as described in Materials and Methods (figure 4.6)

The protein concentration of the standard S-Layer preparations were identified as about 5,66 mg/ml by using the same techniques as described previously for the total protein analysis of bacterial cultures. Standard solutions were diluted in order to obtain 1mg/ml protein solution. Thus, an estimated final protein concentration was obtained by addition of approximately 5ml of 5% SDS solution. For surface coverage experiments, the stock solution was diluted again in 5%SDS to a concentration between 0.1-1mg/ml

4.3. Characterization Results of Electropolished Aluminum Surfaces

4.3.1. Optical Profilometer Results

The surface roughness values of aluminum before electropolishing were in the order of 800nm to 1um. After electropolishing, surface roughness values were decreased to 80-150nm. Results obtained via optical profilometer indicates that applied electropolishing process was very effective since it decreases considerably the

surface roughness. Moreover, electropolishing time and temperature were also optimized according to the profilometer results. The optimum electropolishng time was determined between 5 to 7 minutes. The electrolyte temperature was adjusted to approximately 90°C. It has also been determined that without vigorous shaking oxygen bubbles forms on the surface which causes several pits along the surface. Obtaining a pit free surface was a critical condition because in further protein adsorption studies, protein tends to accumulate in the pitted areas.

4.3.2. AFM Investigations

All atomic force microscopy experiments were conducted on a Ntegra Prima AFM under Tapping Mode conditions using amplitude feedback control. Linear scans rates were typically 0.8 – 1.2 μm s^{-1}. Probes were NT-MDT SPM probes with a typical resonance frequency of 250 – 350 kHz and a nominal tip radius of less than 10 nm. Lateral size bars on images are based on calibrations with diffraction grating standards and are accurate to within 1%.

Optical profilometer results were confirmed via AFM. Similar results were obtained and the difference between polished and unpolished surface topographies were clearly seen.

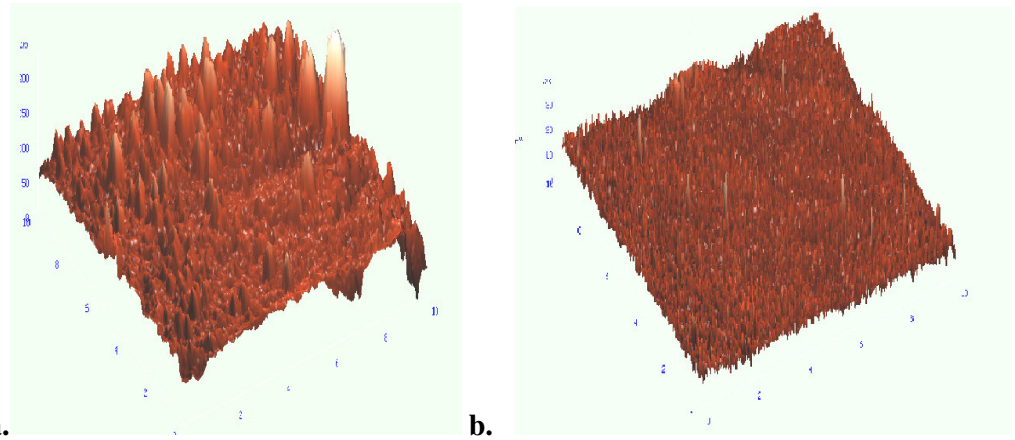

a. **b.**

Figure 4.6: AFM investigations of unpolished (a) and polished (b) surfaces

The surface roughness of aluminum samples were about 700nm and 1um prior to electropolishing. Since the samples were going to be used as substrates in protein coverage experiments, an extremely flat and smooth surface was needed. Figure 4.6 shows the difference between polished and unpolished samples' surfaces in three dimensions. After electropolishing the surface roughness of the same samples have

been decreased to roughly 100nm and below. The surface roughness of the sample in figure 4.6b was determined via AFM investigations as 78 nm. Prior to electropolishing the same area had a roughness in the order of 335 nm.

4.4. Crystallization of S-Layer Proteins on Inorganic Surfaces

4.4.1. Preliminary Experiments on Silicon Wafer and Mica

The intrinsic property of S-layer proteins to form extended crystalline arrays on solid supports is one of the most important features for functionalizing surfaces. Recrystallization of S-layer proteins were first accomplished on silicon wafer and mica surfaces. Those materials have the common property to posses an extremely flat and easy to clean surfaces. Thus a strong protein adsorption and a good pattern formation on the surface of these materials were expected. The experiments performed on silicon wafer and mica had also the aim of confirming the quality of purified proteins and the aim of optimizing atomic force microscopy conditions to visualize s-layer patterns. All patterning experiments either on silicon wafer, mica or aluminum were conducted at room temperature.

a) AFM Studies on Silicon Surface

The recrystallisation of S-layer proteins on silicon wafer substrates has been studied by atomic force microscopy (AFM). AFM studies realized on Si wafer surfaces revealed a partial monolayer coverage. S-layer proteins form extended monolayers on native silicon surfaces as seen in figure 4.8. Hence to obtain surface patterns via s-layer proteins there is no need of chemically modifying the surfaces. No regularity was observed either on surface coverage percentages or monolayer or multilayer formation of recrystallized proteins. Figure 4.8 shows an example of monolayer coverage, while figure 4.9 shows a multilayered coverage on different areas of the same sample. Since it is the same sample the contact time between the protein stock solution and the substrate was equal on both regions. Thus, it can be concluded basing on those results that the contact time of the substrate with the protein solution does not have an influence on generating either a monolayer or a multilayer pattern.

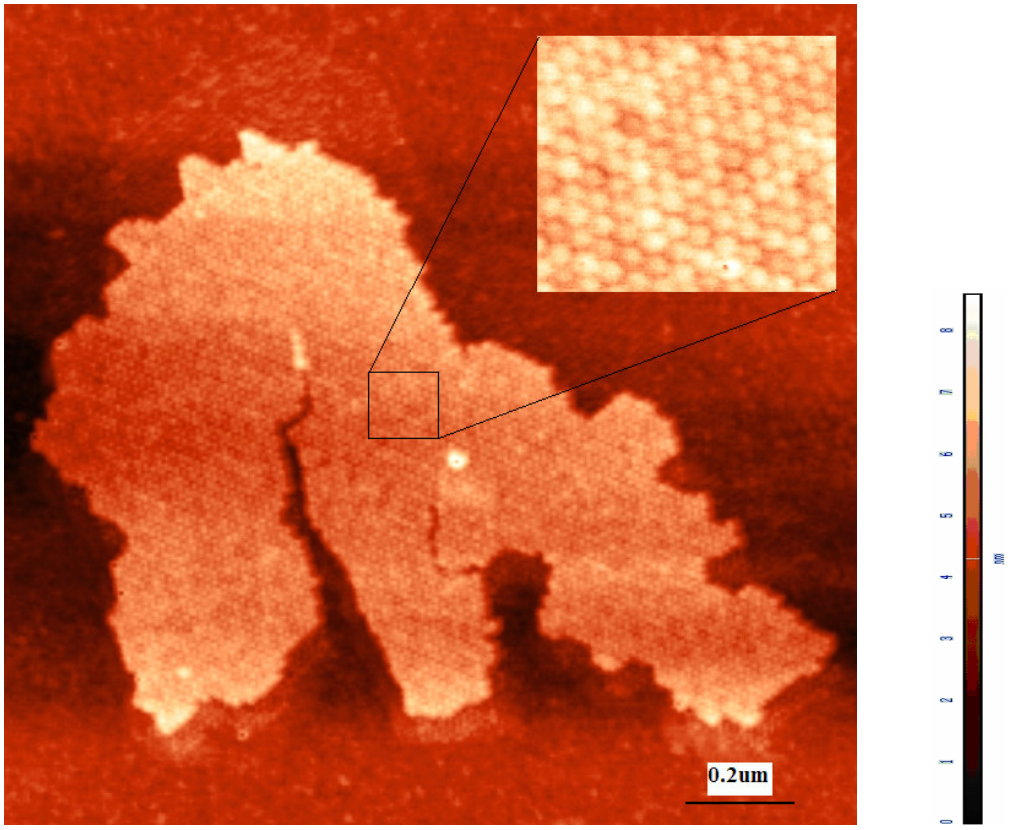

Figure 4.7: Tapping mode AFM image of HPI layer proteins on silicon wafer reveals a monolayer coverage when they are immersed into the protein containing solution for several minutes before washing.

A typical surface coverage take place after more or less 15 to 60 min of substrate contact time with the stock protein solution. Multilayer formation is more abundantly observed when contact times exceeded 60 minutes. Hence, The time required for the optimum coverage was determined as 60 minutes.

It is also important to notice that the surface coverage occurs in form of small patches on the substrate and it does not follow a regular arrangement along the surface. The surface area of patterns formed on the surface does not exceed 1µmx1µm (and even it is often smaller). This can be explained by the fact that the proteins are extracted intact from the native bacteria, and the size of a is in the order of few micrometers hence it is not likely to get fragments larger than that size.

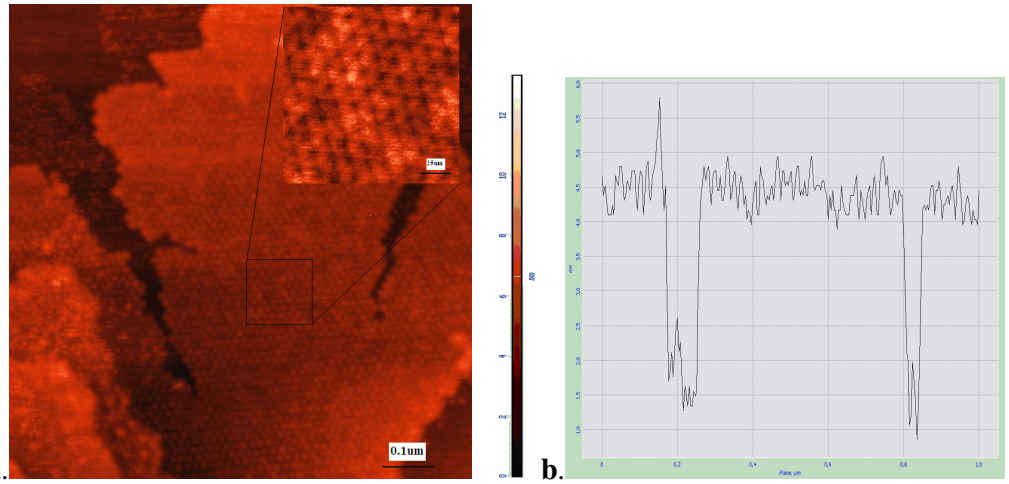

Figure 4.8: a) Semi contact imaging mode AFM images of a partially multilayered patterns on silicon wafer surface. b) Line profile of the s-layer coating on the silicon wafer

AFM examination of partially covered surfaces as seen in Figure 4.9a and 4.9b shows that protein monolayers are 5-6 nm in height with single-crystal domain cluster sizes of around 1 μm as observed in the other similar studies in the literature.. Multilayering of the S-layer structures can not be totally eliminated. There is not any method developed yet for the elimination of this multilayering.

b) AFM Studies on Mica Surface

Mica surface constitutes an ideal substrate material for protein coverage experiments because it becomes fresh, clean and atomically flat after each cleavage procedure. The mica surface was cleaved using Scotch® tape. Protein coverage experiments on mica surface revealed that for flatter surfaces the pattern formation occurs very quickly (even in a few minutes) and monolayer formation was more abundant than multilayer covered areas (Figure 4.10). The S-layer patterned surface area also increases proportionally with improved surface properties but is still limited to a mximum area of approximately $1\mu m^2$ (Figure 4.12)

The hexagonal patterns of HPI layer proteins were observed very easily on the mica surface. The height profile seen in the figure 4.11 results indicate that the thickness of the monolayer is about 9nm.

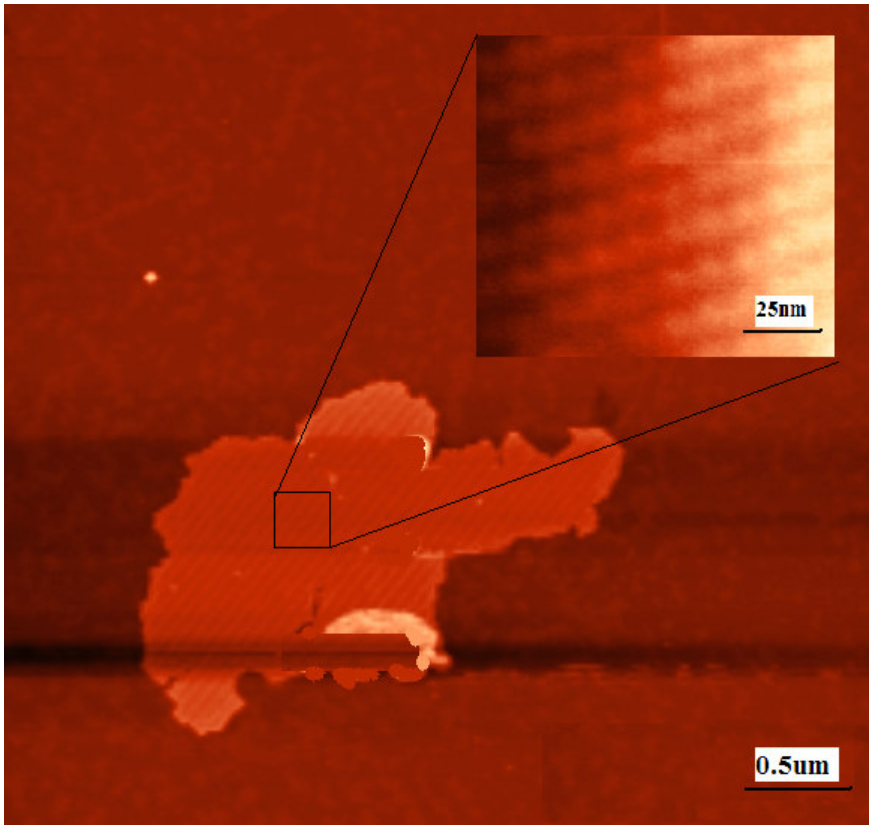

Figure 4.9: Tapping mode AFM image of HPI layer proteins on freshly cleaved mica surface. A monolayer coverage occurs as small patches when proteins are contacted to the substrate for several minutes before washing.

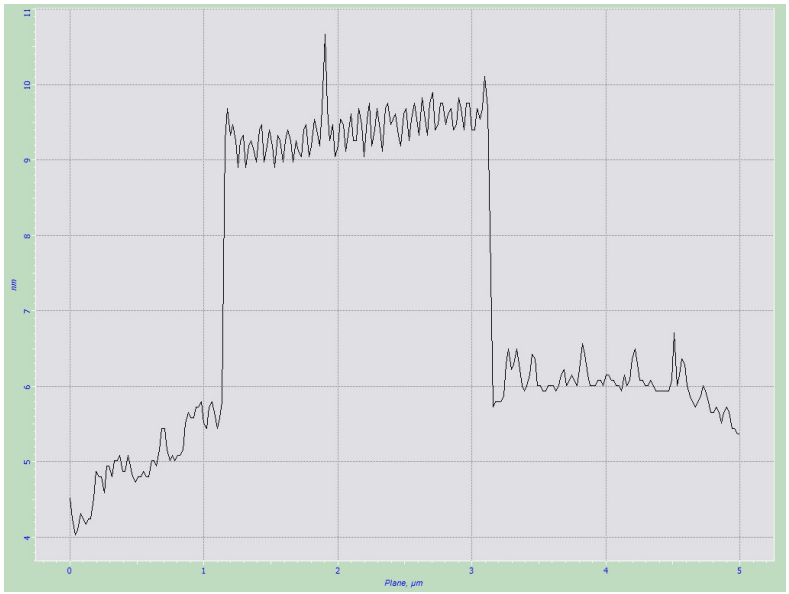

Figure 4.10: Height profile of HPI layer proteins adsorbed on mica surface. The thickness of HPI layer proteins are alomost 10nm which is adequate with the previous studies.

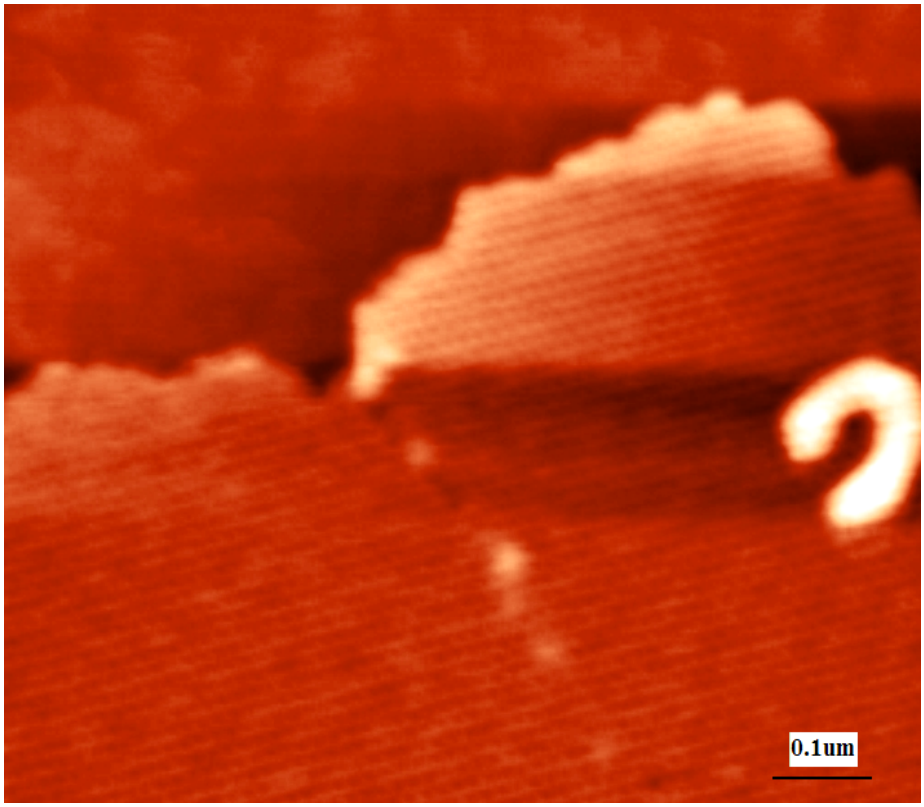

Figure 4.11: Semi contact mode AFM image of HPI layer proteins on freshly cleaved mica surface.

4.4.2. Nanopattern Formation on Aluminum Surface via S-layer Proteins

Electropolished aluminum surfaces were first cleaned with alcohol and than deionized water by utrasonication. About 20-40 μL cm^{-2} of stock HPI layer solution (0.1-1 mg mL^{-1}) was applied onto the surface by pipet. The solution was left to air dry for complete coverage which takes approximately 60 minutes. When the drying is complete the surface was repeatedly immersed in ddH_2O followed by air drying via nitrogen blow.

On aluminum surfaces a combination of mono and multi layer coverage is observed (Figure 4.13) General covered area on aluminum is lower when compared to both mica and silicon surfaces. Monolayered and multilayered areas are found to be overlapped on each other and often multilayer parts are located at the center of covered areas (figure 4.14). Figure 4.15 shows intact hexagonal surface layer proteins that are self-assembled on aluminum surface and on which a nanopattern formation is clearly observed.

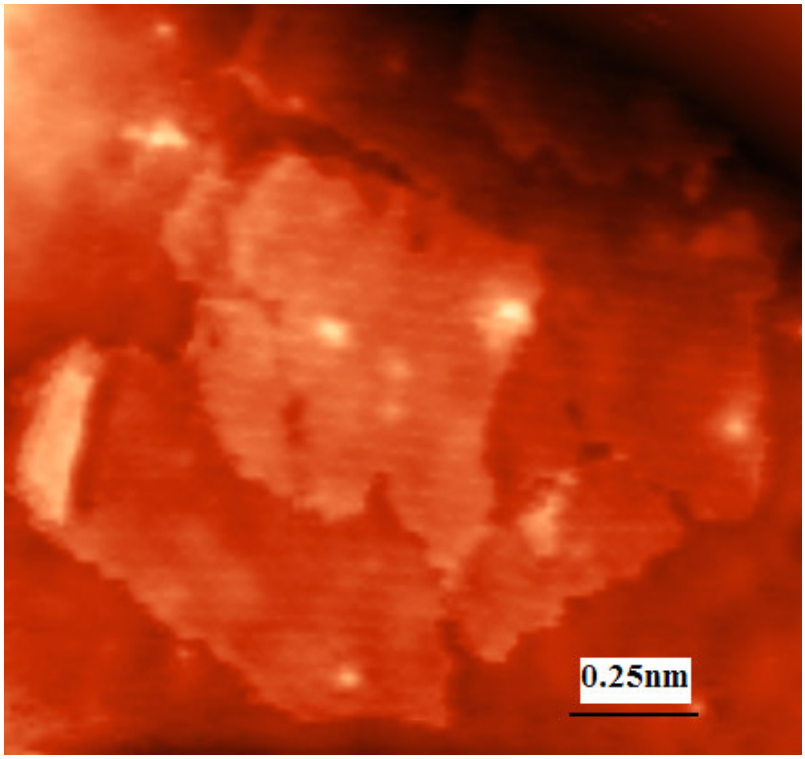

Figure 4.12: Tapping mode AFM image of HPI layer proteins adsorbed electropolished aluminum surface

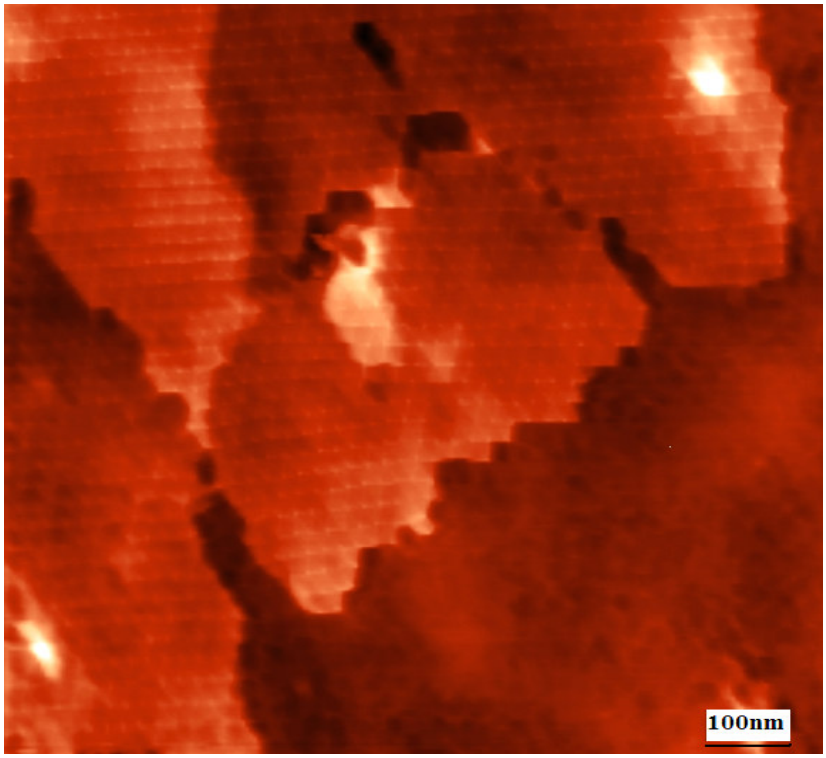

Figure 4.13: Tapping mode AFM image of HPI layer proteins on aluminum surface. Multi and monolayer adsorptions are overlapped.

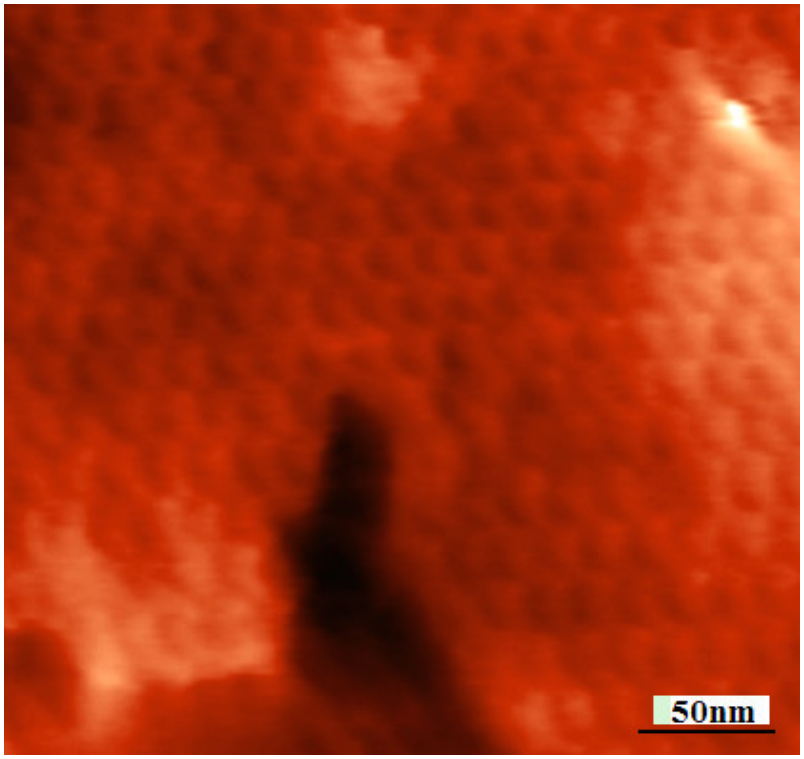

Figure 4.14: Tapping mode AFM image of HPI layer proteins on aluminum surface. Hexagonal structure of recrystallized s-layers are seen clearly.

The experiments accomplished so far have successfully demonstrated that the formation of coherent crystalline arrays occurs on silicon wafer, mica and aluminum surfaces. Furthermore the conditions of the crystallization solution and on the surface properties of the substrate affect strongly the crystallization properties. Concerning the surface properties of the substrate, minimizing the roughness is sufficient to obtain a good s-layer coverage.

Pore openings are uniform on each of the substrates, which leads to the assumption that those materials can be used arrays for further material processing.

Multilayer coverage does not affect the material properties if it is expected to be used as a nanomask [4].

5. CONCLUSION

In conclusion, interconnecting nature's ability to form self-assembled structures for novel engineering and biotechnology applications is an attractive alternative to conventional fabrication methods. The HPI layer from *Deinococcus radiodurans*, previously demonstrated to be able to form nanopatterns on various substrates is herein investigated further as a potential for biopatterning surfaces at nanometer scale for synthesis of ordered nanostructured arrays.

In this study, it is demonstrated that S-Layer proteins of Deinococcus *radiodurans* forms regular arrays of hexagonal structures with uniform pore openings on various inorganic substrates. Since the *D. radiodurans* HPI layer is a robust protein that remains structurally intact under a wide range of environmental conditions its homogenous pore areas allows further processing of the material by using S-layer proteins as a mask either for nanoparticle deposition or as a template for nanotemplate. We demonstrated that the formation of relatively large crystalline arrays by S-layer proteins to be utilized as nanomask on the surfaces into which different materials can be deposited.

The formation of coherent crystalline arrays strongly depends on the specific S-layer protein used, on the conditions of the crystallization solution and on the surface properties of the substrate. Concerning the surface properties of the substrate, it is safe to say that extremely flat surfaces are often required for uniform crystal growth but they are not strictly necessary. It is also a fact that atomically flat surfaces such as mica favorises S-layer recrystallization on larger areas. On the other hand, careful control of the deposition thickness and nucleation properties are necessary to achieve uniform surfaces. Thus, the repeatable synthesis of large-area, perfectly ordered nanoarrays under such conditions remains a technical challenge

Finally, for further future, the possibility to change the natural properties of S-layer proteins by genetic manipulation is considered to be a new challange for the tuning of their structural and functional features all together with material properties.

REFERENCES

[1] **Tamerler C, and Sarikaya M**, 2007, Molecular biomimetics: Utilizing nature's molecular ways in practical engineering, *Acta Biomater*, doi:10.1016/j.actbio..10.009

[2] **Lin, B**., 2006, Optical lithography-Present And Future Challenges, *C. R. Physique,* **7,** 858–874

[3] **Sarıkaya, M., Tamerler, C., Y.jen, A.K, Schulten,K., and Baneyx, F.,** 2003. Molecular Biomimetics: Nanotechnology Through Biology, *Nature Materials*, **2**, 577-585.

[4] **Allred, D., Sarikaya, M., Baneyx, F., and Schwartz, D**.; 2005, Electrochemical Nanofabrication Using Crystalline Protein Masks**,** Nano Letters, 609-613

[5] **Sleytr, U.B.,** 1997, Basic and applied s-layer research: overview*, FEMS microbiology reviews*, 5-12,

[6] **Baumeister, W., Karrenberg, F., Rachel,R., Engel,A., Ten Heggeler,B., and Saxton, W.O**.; 1982, The Major Cell Envelope Protein of Micrococcus radiodurans*, Eur. J. Biochem.* ***125****,* 535-544

[7] **Sarıkaya, M. and Tamerler, C.,** Molecular Biomimetics: Linking Polypeptides to Inorganic Structures, *Tools for Bionanotechnology*, 191-221

[8] http://www.nature.com/nature/journal/v437/n7059/pdf/nature04166.pdf

[9] **Postek, M.T.**,2004, National Institute of standards and technology workshop, *National nanotechnology initiatice workshop report*, Gaithersburg, Mayland,US

[10] **Lei, Y., Cai, W. and Wilde, G**.; 2007, Highly ordered nanostructures with tunable size, shape and properties: A new way to surface nano-patterning using ultra-thin alumina mask*, Progress in Materials Science*, **52**, 465–539

[11] http://www.cise.columbia.edu/clean/process/Photolithography_Lessons.pdf

[12] http://en.wikipedia.org/wiki/Photolithography

[13] **Hawryliw, A**.; 1997, Pattern Generation For The Next Millennium, *Microelectronic Engineering*, **35**, 501-507

[14] **Hsieh, K. and Leslie, E.,** *2005,* Electron-Beam Lithography and X-ray Lithography*; ENEE 416 – Group Activity #2,*

[15] **Gierak, J**., 2005, Exploration of the ultimate patterning potential achievable with focused ion beams*, Microelectronic Engineering*, **78–79**, 266–278

[16] **Kemp,K. and Wurm, S**., 2006, EUV lithography, *C. R. Physique***, 7**, 875–886

[17] **Haffner, M., Heeren, A., Fleischer, M., Kern,D.P., Schmidt, G.; and Molenkamp, L**., 2007, Simple high resolution nanoimprint-lithography, *Microelectronic Engineering*, **xxx,** xxx–xxx

[18] **Truskett,V. and Watts,M**., 2006, Trends in imprint lithography for biological applications, *Trends in Biotechnology*, **24,** 7

[19] **Xie, X.N., Chung, H.J., Sow, C.H. and Wee, A.T.S.**, 2006, Nanoscale materials patterning and engineering by atomic force microscopy nanolithography*, Materials Science and Engineering*, **54**, 1–48

[20] **Aissou, K., Kogelschatz, M., Baron, T. and Gentile, P.**, 2007, Self-assembled block polymer templates as high resolution lithographic masks*, Surface Science,* **xxx**, xxx–xxx

[21] **Choi D., Kyun Yu,H., and Yang, S.,** 2004, 2D nano/micro hybrid patterning using soft/block copolymer lithography*, Materials Science and Engineering*, **24**, 213–216

[22] **Shimomuraa,M. and Sawadaishib, T**., 2001, Bottom-up strategy of materials fabrication: a new trend in nanotechnology of soft materials*, Current Opinion in Colloid & Interface Science,* **6**, 11-16

[23] **Sleytr, U.B., Messner, P., Pum,D., Sara,M., Schuster, B. and Schaffer, C**.; 2004, Self-assembly Protein Systems: Microbial S-layers, *Biopolymers,* **7,** Weinheim Germany

[24] **Sleytr, U.B., and Beveridge**,**T.J.,** 1999, Bacterial S-layers, *Trends in Microbiology* ,**7,** 253-260

[25] **Rachel, R., Pum, D., Smarda, J., Riegger, G., Smajs, D. and Stetter, K**., 1997, Fine structure of s-layers*, FEMS microbiology reviews*,**20**, 13-23

[26] **Sleytr, U.B**.,1997, Basic and applied s-layer research: overview, *FEMS microbiology reviews*,**20,** 5-12

[27] **Sleytr, U.B., Messner, P., Pum,D. and Sara,M**.; 1999, Crystalline Bacterial Cell Surface Layers (S Layers): From Supramolecular Cell Structure to Biomimetics and Nanotechnology, Angew. Chem. Int. Ed., **38**, 1034 ± 1054

[28] **Sleytr, U.B. and Sara, M.**, 1997, Bacterial and archaeal S-layer proteins: structure-function relationships and their biotechnological applications, *Tibtech* review,**15,** 20-26

[29] **Sleytr,U.B., Huber, C., Ilk, N., Pum,D., Schuster, B. and Egelseer, E**.;2007, S-layers as a tool kit for nanobiotechnological applications , *FEMS Microbiol Lett*, **267**, 131–144

[30] **Sleytr, U. B., Sara, M., Dietar, P., and Schuster, B**.; 2001, Characterization and use of crystalline bacterial cell surface layers*, Progress in surface science*, **68**, 231-278

[31] **Pum,D., Neubauer,A., Gyoervary,E. Sára,M., and Sleytr,U.B.**,2000, S-layer proteins as basic building blocks in a biomolecular construction kit, *Nanotechnology,* **11**, 100-107

[32] **Sleytr, U.B., Messner, P., Pum,D. and Sara,M.**, 1999, Crystalline Bacterial Cell Surface Layers (S Layers): From Supramolecular Cell Structure to Biomimetics and Nanotechnology, *Angew. Chem. Int. Ed*., **38** , 1034 ± 1054

[33] **Shenton, W., Pum, D., Sleytr, U.B. and Mann, S**.; Synthesis of cadmium sulphide superlattices using self-assembled bacterial S-layers, *Nature*, ,**389**, 585-587

[34] **Dieluweit, S, Pum, D., Sleytr, U.B. and Kautek,W**., 2005, Monodisperse gold nanoparticles formed on bacterial crystalline surface layers (S-layers) by electroless deposition, *Materials Science and Engineering*, **25**, 727 – 732

[35] **Küpcü, S., Mader, C., Weigert, S., Unger, F., Messner, P., Schimid, B., Schuster, B., Pum,D., Douglas, K., Clark, N., Moore, T., Winningham, T., Levy, S., Frithsen, I., Pankovc, J., Beale, P., Gillis, H., Choutov, D. and Martin, K**., 1997, Application of S-layers, *FEMs Microbiology Reviews,* **20**, 151-175

[36] **Battista, J.R.; Earl, A.; Park, M.;** "Why is *Deinococcus radiodurans* so resistant to ionizing radiation?", Trends in Microbıology 362 VOL. 7 NO. 9 , 1999

[37] **Mattimore, V. and Battista, J.R**., 1996, Radioresistance of *Deinococcus radiodurans*: Functions Necessary To Survive Ionizing Radiation Are Also Necessary To Survive Prolonged Desiccation, *Journal of Bacterıology*, **178**, 633–637

[38] **Sidhu,M.S. and Olsen, I**., 1997, S-layers of Bacillus species, *Microbiology*, **143**, 1039–1052

[39] **Aggave Biosystems,** Product catalogue, S-layers

[39] **Whitesides,G.M**.,2002, Self Assembly At All Scales, *Science,* **295**, 2418

[40] **Fung,S.Y., Hong, Y., Baig, C.K. and Chen,P**.,2005, Self-assembly of peptides and its potential applications*, Woodhead Publishing Limited*, NY

[41] **Shuguang Zhang**, 2002, Emerging biological materials through molecular self-assembly, *Biotechnology Advances*, **20**, 321–339

[42] **Zhao, X. and Zhang, S**., 2007, Designer Self-Assembling Peptide Materials, *Macromoecular Bioscience,* **7**, 13–22

[43] **Zhang, S., Marini, D., Hwang, W. and Santoso, S**., 2002, Design of nanostructured biological materials through self-assembly of peptides and proteins, *Current Opinion in Chemical Biology*, **6**, 865–871

[44] **Schulz, E., Bandelmann, R., Escherich,V., Keese, V., Leenen, M., Lilje, L. Matheisen, A., Morales, H., Schmüser, P., Seidel, M., Steinhau-Kühl, N, and Tiessen, J.,** 2001, Engineering Solutions For The Electro-Polishing Of Multi-Cell Superconducting Accelerator Structures, *Proc. SRF2001,* Tsukuba, Ibaraki, Japan, 481

[45] **Eozenou F., Antoine C., Aspart, A. Berry, S. Denis, JF. and Malki B.**; Efficiency of electropolishing versus bath composition and Aging: first results

[46] **Terryn, H**., Aluminium Surface Pretreatment, TALAT Lecture 5201

[47] **Möller, P.**, Surface Treatment of Aluminium, TALAT Lecture 5105

[48] **Wang,X. and Han, G.,**2003, F abrication and characterization of anodic aluminum oxide template, *Microelectronic Engineering,* **66**, 166–170

RESUME

Zehra Beril Akıncı was born in Istanbul in 1981. After getting her high school diploma from Saint Benoit French High School in 2000, she started to study in Istanbul Technical University, Department of Metallurgical and Materials Engineering in 2000. She graduated in 2005 and at the same year, she was accepted to Materials Engineering Master's program in Department of Materials Science and Engineering. She is still pursuing her studies in the same department.